arXiv:2512.02895v2 [cs.CV] 3 Dec 2025

MindGPT-4ov: An Enhanced MLLM via a Multi-Stage Post-Training Paradigm

MindGPT-4o Team, Li Auto Inc.

Abstract

We present MindGPT-4ov[1], a multimodal large language model (MLLM) that introduces a general post-training paradigm spanning data production, model training, and efficient deployment. It achieves state-of-the-art performance across multiple benchmarks at low cost, effectively enhancing the foundational capabilities of MLLMs and the generalization ability. Focusing on data construction, supervised fine-tuning strategies, and multimodal reinforcement learning methods, this work proposes three key innovations: (1) An information density-based data generation scheme, integrated with a dual-dimensional tree-structured label system, enabling automated generation of high-quality cross-domain data. (2) A collaborative curriculum supervised fine-tuning approach that balances the injection of domain-specific knowledge with the preservation of general capabilities. (3) A hybrid reinforcement learning paradigm that enhances reasoning ability while simultaneously addressing multi-objective optimization such as diversity exploration, maintenance of multimodal perception, and response conciseness. Moreover, we implement a series of infrastructure optimizations, such as 5D parallel training, operator optimization, and inference quantization to enhance training and inference efficiency while reducing the cost of domain adaptation. Experimental results demonstrate that the MindGPT-4ov model outperforms state-of-the-art models on benchmarks such as MMBench, MMStar, MathVision, and MathVista. In addition, MindGPT-4ov also demonstrates superior user experience in vertical domain tasks, enabling a seamless transition from academic research to industrial deployment. MindGPT-4ov provides a general post-training paradigm applicable to a wide range of MLLMs. The model weights, datasets, and code for the Qwen3-VL-based variants will be recently open-sourced to support the community's development of MLLMs.

1 Introduction

In recent years, multimodal large language models (MLLMs) have achieved breakthrough progress in vision–language understanding (Comanici et al., 2025; Guo et al., 2025b; Zhu et al., 2025; Bai et al., 2025b,a), demonstrating powerful general perception and reasoning capabilities, which have reached unprecedented performance in tasks such as image understanding, visual question answering, and document analysis. A key challenge in current MLLM development is how to effectively transfer general multimodal capabilities to vertical applications while maintaining strong generalization, such as in autonomous driving (Tian et al., 2024; Hegde et al., 2025), embodied intelligence (Zhou et al., 2025; Cai et al., 2025b; Chen et al., 2024a), and medical

---

[1] MindGPT-4o-v(ision) is the visual component of the MindGPT-4o project led by the foundation model team at Li Auto Inc., which is a multimodal large language model built on MindGPT.

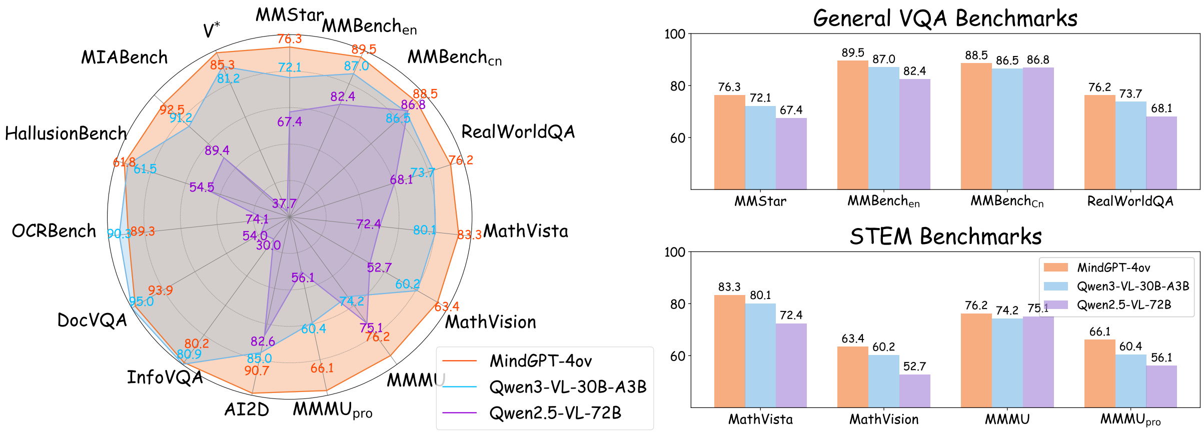

Figure 1 Performance of MindGPT-4ov across multiple benchmarks.

intelligence (Lin et al., 2025; Lozano et al., 2025). To address this challenge, some studies have explored various lines of exploration. For example, SpatialBot (Cai et al., 2025b) applies MLLMs to embodied intelligence, helping robots perceive their environment and plan tasks; DiMA (Hegde et al., 2025) proposes an end-to-end autonomous driving system distilled from a pre-trained MLLM; and HealthGPT (Lin et al., 2025) is an MLLM used to support medical treatment.

However, these studies suffer from two problems, resulting in poor practicality and generalization of current models: (1) as MLLMs acquire domain expertise, they often suffer from catastrophic forgetting, degrading their original general understanding capabilities; and (2) they lack a systematic post-training methodology: they either prioritize domain data collection while neglecting stringent data quality and cost controls; focus solely on learning domain-specific capabilities at the expense of maintaining foundational general abilities and real-world user experience; or optimize the training framework without adequately accounting for practical deployment requirements.

By contrast, we propose the MindGPT-4ov framework that offers a systematic, end-to-end methodology that covers the entire pipeline, including: **(1) An information density-driven data synthesis method.** Through automated data acquisition, intelligent annotation assistance, and data quality assessment, we build high-quality training sets with data augmentation and synthesis strategies to alleviate long-tailed data distributions; **(2) A collaborative curriculum supervised fine-tuning method.** This framework integrates domain expertise into the model through coordinated data admission techniques and curriculum learning, which preserves its general capabilities and applies targeted optimizations to address user-experience pain points. **(3) A multi-stage hybrid-reward reinforcement learning method.**Through multi-stage reinforcement learning, combined with a carefully designed hybrid reward strategy, we progressively improve both general and vertical domain performance. **(4) A 5D parallel training framework.** For Mixture-of-Experts (MoE) architectures (Cai et al., 2025a), we introduce a series of training optimizations during the supervised fine-tuning and reinforcement learning phases to significantly improve training efficiency. We also optimize the inference engine to enhance the user experience in high-concurrency and other specific application scenarios.

Ultimately, the model trained with the proposed framework not only excels on vertical applications but also preserves or even enhances general performance, all while providing an enhanced user experience. To be specific, our model performs competitively on general multimodal benchmarks, matching or surpassing state-of-the-art Qwen3-VL-30B-A3B (Bai et al., 2025a) across nearly all metrics. In particular, as shown in Fig. 1, it exceeds Qwen3-VL-30B-A3B by an average of 3.4% on general VQA benchmarks and by an average of 3.6% on math and STEM (Science, Technology, Engineering, Mathematics) benchmarks, respectively. In addition, it also provides a superior real-world user experience, such as . Finally, the proposed framework supports efficient deployment, characterized by lower CPU/GPU utilization, more efficient cache reuse, faster response times, and improved user experience.

In summary, MindGPT-4ov's end-to-end, systematic design ensures that data preparation, model training, and deployment are all optimized, enabling a seamless transition from academic research to industrial application. Our main contributions include:

- ***A generalizable post-training paradigm.*** We propose MindGPT-4ov, whose training paradigm is applicable to most current MLLMs. Our approach encompasses high-quality data construction, a multi-stage supervised fine-tuning and reinforcement learning scheme, and efficient training and deployment strategies, providing a low-cost, reusable, and scalable technical pathway for the real-world deployment of MLLMs.
- ***Outstanding performance.*** The MindGPT-4ov model achieves superior performance across multiple multimodal general benchmarks compared to Qwen3-VL. Moreover, it can provide a better user experience for the specific domain tasks than Qwen3-VL.
- ***Open-source release.*** We will recently open-source parts of the code and data and models, enabling the community to build on this foundation and extend the models' capabilities in specific vertical applications.

2 Data Construction

2.1 Challenges

In the transition from general MLLMs to vertical applications, constructing high-quality training data often encounters several thorny challenges, mainly including: (1) Producing high-quality data is costly and resource-intensive, overly reliant on manual annotation, and lacks automated pipelines for high-quality data generation. (2) Training data distributions are often imbalanced: insufficient vertical-domain knowledge data impairs generalization, while a shortage of general multimodal data risks degrading core multimodal capabilities. (3) Data produced by conventional pipelines often lacks diversity, making it difficult to comprehensively expand multimodal capabilities under limited data budgets. (4) Vertical-domain data is typically expensive to acquire and relatively scarce, and standard data production methods struggle to unlock the potential value of such scarce data.

2.2 Solution

To address the aforementioned challenges and better support the transition of general-purpose MLLMs to vertical-specific MLLMs, we propose a comprehensive data construction framework, which is presented in Fig. 2. The specific innovations are as follows: We firstly present a dual-dimensional tree-structured label system. This system is designed to balance vertical knowledge coverage and general capability adaptation, which provides the direction for generating data with broad coverage, high diversity, and balanced distribution, while also offering clear guidance for model iteration and evaluation. Then, we develop a data synthesis pipeline based on an information density. Different quantitative systems are designed for static image features, enabling the accurate capture of the potential value of data through weighted fusion. This allows for dynamic adjustment of the quantity of generated QA (question-answer) pairs.

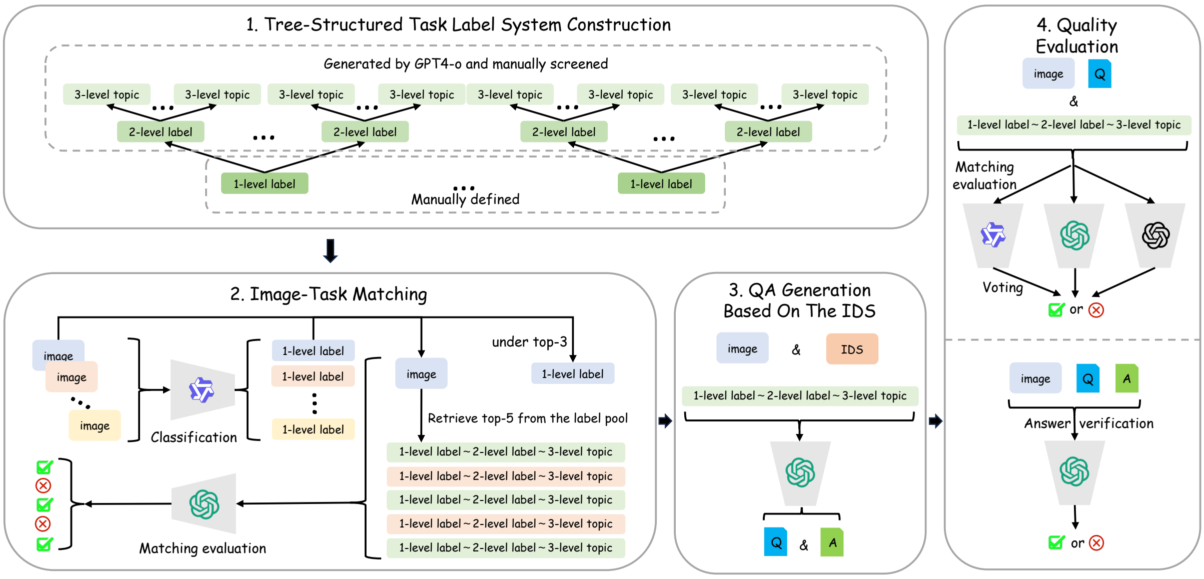
1. Tree-Structured Task Label System Construction
Generated by GPT4-o and manually screened
3-level topic
2-level label
1-level label
Manually defined
2. Image-Task Matching
image
Classification
1-level label
under top-3
Retrieve top-5 from the label pool
1-level label ~ 2-level label ~ 3-level topic
Matching evaluation
3. QA Generation Based On The IDS
image
&
IDS
1-level label ~ 2-level label ~ 3-level topic
Q
A
4. Quality Evaluation
image
Q
&
1-level label ~ 2-level label ~ 3-level topic
Matching evaluation
Voting
or
image
Q
A
Answer verification
or

Figure 2 An overview of our data pipeline. We begin by constructing a tree-structured hierarchical label system. We then employ MLLMs to match images with their corresponding task labels. An MLLM is subsequently prompted to generate question–answer pairs based on the images, the task labels, and the information density score (IDS). Lastly, MLLMs are leveraged for matching evaluation and answer verification to ensure data quality.

The proposed data production scheme improves upon the coarse-grained indiscriminate resource allocation typical of traditional data synthesis. By generating more high-value data and investing less in low-value data, our method balances resource expenditure while fully tapping the potential of high-quality data. It addresses common challenges in multimodal data production, including low efficiency, poor quality, limited coverage, and imbalance, consistently producing diverse, well-balanced, and highly accurate data, thereby providing an efficient and reliable paradigm for multimodal data generation.

2.2.1 Dual-dimensional Label System

To simultaneously support vertical domain knowledge coverage and general capability maintenance, the label system is designed around two dimensions: **domain** and **ability**.

- Domain dimension covers vertical domain knowledge across automotive, healthcare, education, industry, daily life, and others, anchoring each datum to concrete application scenarios to ensure the synthesized data aligns with target domains.
- Ability dimension focuses on the general abilities of MLLMs, primarily encompassing image-related dimensions such as OCR, counting, spatial perception, logical reasoning tasks, and others.

The dual-dimensional design offers the advantage of breaking through the limitations of traditional single-dimensional label systems. It enables each synthesized data sample to be associated with specific vertical domain knowledge while simultaneously addressing explicit model ability training requirements. This establishes a foundation for subsequent multimodal training data synthesis. The comprehensive and diverse domain labels help guide the data production in synthesizing domain knowledge tailored to various verticals. Decoupling knowledge from ability also allows the training process to better understand data distribution, facilitating adjustments in data

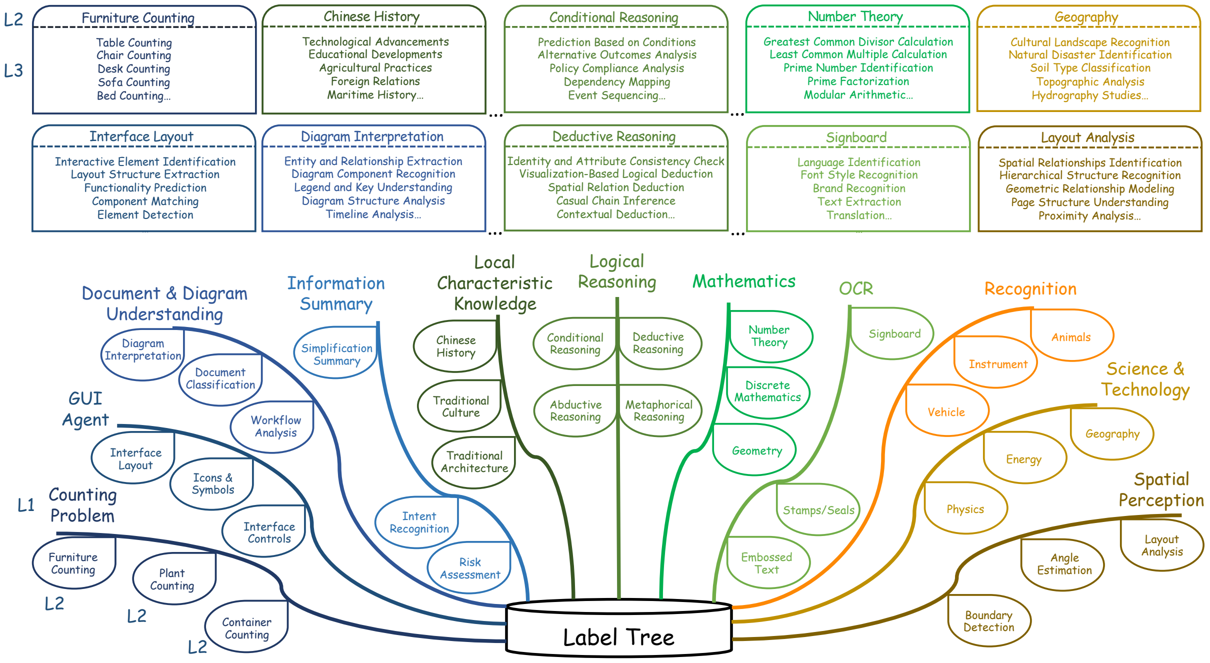
L2
L3
Furniture Counting
Table Counting
Chair Counting
Desk Counting
Sofa Counting
Bed Counting...
Chinese History
Technological Advancements
Educational Developments
Agricultural Practices
Foreign Relations
Maritime History...
Conditional Reasoning
Prediction Based on Conditions
Alternative Outcomes Analysis
Policy Compliance Analysis
Dependency Mapping
Event Sequencing...
Number Theory
Greatest Common Divisor Calculation
Least Common Multiple Calculation
Prime Number Identification
Prime Factorization
Modular Arithmetic...
Geography
Cultural Landscape Recognition
Natural Disaster Identification
Soil Type Classification
Topographic Analysis
Hydrography Studies...
Interface Layout
Interactive Element Identification
Layout Structure Extraction
Functionality Prediction
Component Matching
Element Detection
Diagram Interpretation
Entity and Relationship Extraction
Diagram Component Recognition
Legend and Key Understanding
Diagram Structure Analysis
Timeline Analysis...
Deductive Reasoning
Identity and Attribute Consistency Check
Visualization-Based Logical Deduction
Spatial Relation Deduction
Casual Chain Inference
Contextual Deduction...
Signboard
Language Identification
Font Style Recognition
Brand Recognition
Text Extraction
Translation...
Layout Analysis
Spatial Relationships Identification
Hierarchical Structure Recognition
Geometric Relationship Modeling
Page Structure Understanding
Proximity Analysis...
Document & Diagram Understanding
Diagram Interpretation
Document Classification
Workflow Analysis
Information Summary
Simplification Summary
Intent Recognition
Risk Assessment
Local Characteristic Knowledge
Chinese History
Traditional Culture
Traditional Architecture
Logical Reasoning
Conditional Reasoning
Deductive Reasoning
Abductive Reasoning
Metaphorical Reasoning
Mathematics
Number Theory
Discrete Mathematics
Geometry
OCR
Signboard
Stamps/Seals
Embossed Text
Recognition
Animals
Instrument
Vehicle
Science & Technology
Geography
Energy
Physics
Spatial Perception
Layout Analysis
Angle Estimation
Boundary Detection
GUI Agent
Interface Layout
Icons & Symbols
Interface Controls
L1
Counting Problem
Furniture Counting
Plant Counting
Container Counting
L2
L2
L2
Label Tree

Figure 3 The tree-structured label system. In the label tree, each branch denotes a first-level label, while the leaves represent a selection of corresponding second-level labels. The box diagrams above the tree illustrate representative third-level topics encompassed by certain second-level labels.

allocation during training and ensuring both domain-specific adaptation and the retention of general multimodal capabilities.

2.2.2 Topic Tree

Inspired by (Chen et al.), to address the limited coverage and insufficient richness of manually constructed labels of training data, as shown in Fig. 3, we construct a topic tree through an expert-defined taxonomy and model-based label expansion. Based on the dual dimensions, we construct corresponding two-level labels and ensure their reliability through human curation, forming a foundational knowledge and ability label system. Building upon the two-level labels, we leverage MLLMs to construct topics that combine domain knowledge and abilities, aiming to comprehensively cover the specific applications of MLLMs' abilities in vertical domains. Ultimately, we arrive at a tree structure for both domain and ability dimensions: first-level (L_1) $\sim$ second-level (L_2) labels and third-level topic (L_3). The process specifically consists of the following three steps:

(1) Expert definition. Experts manually define the L_1 label for both domain and ability dimensions to ensure reliability and coverage.

(2) Label expansion. We carefully design prompts and leverage GPT-4o (Hurst et al., 2024) to expand L_2labels based on manually defined L_1 labels, aiming to maximize coverage while maintaining decoupled label definitions.

(3) Topic generation. Based on L_1 and L_2 labels, we use GPT-4o to generate more fine-grained L_3 topics, ensuring that each topic reflects the concrete application domains of specific general capabilities, *e.g.*, *Counting Problem* $\sim$ *Symbol/Sign Counting* $\sim$ *Traffic Signal Counting*.

Leveraging the semantic comprehension and generative capabilities of MLLMs, we obtain 38,455

L_3 topics based on predefined L_1 and expanded L_2 labels. The construction of this extensive topic tree has significantly mitigated the limitations of manually defined labels, such as constrained coverage and inadequate richness. Meanwhile, the topics fuse ability and domain knowledge into practical applications, highlighting the close connection between multimodal capabilities and vertical scenarios and providing support for synthesizing rich and diverse data.

2.2.3 Topic Matching

The goal of topic matching is to accurately associate multimodal data with relevant topics, ensuring the precision and effectiveness of synthetic data. This process leverages the inherent content strengths of the data for annotation to prevent scenarios where high-value data results in low-quality QA pairs or misaligned content. Moreover, due to the vast scale and rich content of the topic tree we construct, the matching process ensures from the source that the generated data achieves broad coverage and high diversity. Specifically, we employ a two-stage matching process of coarse-grained matching followed by fine-grained matching, leveraging the powerful comprehension and multimodal retrieval capabilities of MLLMs, and assign each data corresponding topics. The specific approach is as follows:

Coarse-grained matching. We employ high-performance MLLMs, such as Qwen3VL-235B-A22B (Bai et al., 2025a), to perform relevance ranking of L_1 labels, achieving preliminary matching between image content and labels. The procedure is as follows: Provide the image along with the full set of L_1 labels, and include an *Others* category as a boundary for relevance ranking to prevent ambiguously borderline data from being forcibly categorized. Then rank labels by their relevance to the image content and select the Top-3 L_1 labels that fall above the *Others* category.

To validate the accuracy of coarse-grained matching, we construct a small evaluation set in which each image contains 2 or 3 manually annotated L_1 labels. If the Top-3 L_1 labels resulting from the matching process overlap with the annotated labels, the matching is considered valid. Evaluation results show that the coarse-grained matching achieves an accuracy of 89.7%, which provides a reliable foundation for the subsequent fine-grained matching.

Fine-grained matching. Within the scope of the selected L_1 labels, we use a multimodal retrieval model (*e.g.*, Ops-MM-embedding-v1-7B (Ops, 2025)) to compute cross-modal vector similarity between the $L_1 \sim L_2 \sim L_3$ topics and images and retrieve the Top-5 related $L_1 \sim L_2 \sim L_3$ topics as candidate topics for each image.

2.2.4 Information-density-driven Data Synthesis

Acquiring informative vertical domain data is highly challenging, as it is often difficult to accumulate in large quantities. To fully leverage the potential of scarce data, we propose a data synthesis solution driven by **Information Density Score (IDS)**. By quantifying the potential value of each data point, we dynamically adjust the number of generated QA pairs for them, producing more for high-value data and fewer for low-value data. This method proves more resource-efficient than traditional coarse-grained synthesis approaches, which often allocate resources uniformly. Our method prioritizes high-value data while maintaining cost-effectiveness. Furthermore, to ensure high quality of produced data, we implement a multi-model voting mechanism for post-synthesis quality assessment. This significantly reduces the need for manual intervention and provides a foundation for cost-effective synthetic vertical-domain data.

Data synthesis based on IDS. The IDS assesses image data across four dimensions: subject diversity (the granularity and richness of objects and scene elements in the image), spatial relationship of scenes (the complexity of relative positions and hierarchical relationships among objects), OCR text dimension (the richness of textual information in the image), and world knowledge relevance (the density of entity information in the image that requires external knowledge to answer).

We use MLLMs to score candidate images for QA synthesis based on these four dimensions. The scores are then weighted and fused according to the contribution of each dimension. During weight allocation, the contribution of each dimension to multimodal capability is considered in combination with the application scenarios, ultimately resulting in a unified IDS.

The candidate topics obtained through topic matching determine the direction of QA synthesis, while the IDS determines the upper limit of the number of QA pairs to be generated per image. Images with higher IDS yield more QA pairs, while those with lower IDS yield fewer. QA synthesis is guided by carefully designed prompts and generated based on the candidate topics. Special processing is applied to data with existing annotations to ensure that the original annotation information is not lost.

Quality evaluation based on judge voting. To better align images, topics, and questions, we employ three high-performance MLLMs, Qwen3VL-235B-A22B, GPT-4o, and GPT-5 (gpt, 2025), as judges to evaluate whether the topics and questions match the given images. Specifically, each of these three MLLMs provides a score of 0 or 1 to every (image, topic, question) triplet based on its consistency and rationality. Only samples that receive a score of 1 from at least two models are retained.

This voting mechanism effectively reduces evaluation errors and ensures the accuracy of (image, topic, and question) matching. Additionally, the quality of responses is equally critical. Therefore, we further leverage high-performance MLLMs to validate the generated responses. We instruct the MLLMs to evaluate whether the generated responses are rational and consistent with the images based on five dimensions: accuracy, completeness, authenticity, semantic relevance, and detail plausibility. This process allows filtering and retaining data with high-quality responses.

3 Collaborative Curriculum Supervised Fine-Tuning

Traditional supervised fine-tuning (SFT) often relies on randomly mixing large-scale data, which leads to three major problems: (1) Learning is imbalanced between domain knowledge and multimodal capabilities: overemphasis on cross-domain knowledge acquisition can degrade multimodal abilities, while forced reasoning with insufficient domain knowledge leads to hallucinations. (2) It fails to target model weaknesses: coordination between data production and training is inefficient, resources are often spent on already-mastered capabilities, and training costs are high. (3) It is not optimized for user experience in real vertical scenarios, leading to poor user experience.

To address the above issues, we propose a curriculum-learning SFT paradigm that collaborates with data admission. First, we design a flexible data admission scheme applied throughout the training phases, effectively improving the synergy between data production and model training while reducing overall training costs. Next, we introduce a three-stage progressive SFT strategy: we begin with cross-domain knowledge learning and subsequently repair degraded multimodal capabilities. Finally, to mitigate suboptimal user experience in real-world usage, we perform targeted optimizations and improvements. We focus on the following training objectives: (1) Improve vertical knowledge learning, and bridge the model's knowledge gaps in domains. (2) Balance perception and reasoning capabilities learning, and mitigate capability decay caused by cross-domain data distribution differences or insufficient data quality. (3) Improve user experience through customization tailored to specific domains.

3.1 Data Preparation

To support the three-stage curriculum learning process, we split the whole training data into three subsets: **SFT-Knowledge**, **SFT-Ability**, and **SFT-Preference**. These subsets have different focuses: SFT-Knowledge targets the acquisition of new knowledge in vertical domains; the images of the SFT-Knowledge set are sourced from real-world usage scenarios, whose data annotations are obtained using the data synthesis method described in Sec. 2.2. SFT-Ability focuses on enhancing general capabilities. The images of the SFT-Ability set are sampled from open-source datasets. To collect as much of such data as possible, we sample data from a large-scale repository of images from open-source datasets, including Laion (Schuhmann et al., 2021), SA-1B (Kirillov et al., 2023), and others. We use the data synthesis pipeline described in Sec. 2.2 to annotate the collected images. SFT-Preference is responsible for improving the user experience. The data of the SFT-Preference set are sampled from specific domain or open-source datasets.

3.2 Training Recipe

3.2.1 Overview

This chapter focuses on the data admission pipeline for providing high-quality data and the three-stage curriculum-based model training process. These two components work in synergy to collectively optimize the performance of the SFT model.

As shown in Fig. 4, the data admission pipeline begins by performing data balancing and rejection sampling on the collected data. Data balancing is designed to achieve an even distribution of data across different capability dimensions, while rejection sampling is employed to grade the difficulty of the data. Subsequently, both processed data components undergo a data quality evaluation. Furthermore, we have established an engineered validation mechanism for newly introduced data, enabling efficient integration of multi-source new data into the training set to effectively expand its scale.

The three-stage curriculum-based SFT training process consists of three parts: knowledge learning, capability remedying, and preference alignment. Knowledge learning focuses on injecting vertical domain knowledge to equip the model with the ability to solve domain-specific problems; capability remedying aims to recover the model's performance on general tasks; and preference alignment is used to enhance the model's performance in real-world application scenarios and improve the user experience.

3.2.2 Data Admission

Fine-tuning MLLMs typically require combining diverse data sources from both general and vertical corpora, making it difficult to find an effective data-mix ratio that achieves balance. At the same time, vertical data across domains are heterogeneous and vary widely in quality, so efficiently screening data quality is one of the challenges in training iterations. In practice, model training and data production often proceed in parallel; both sides need close, efficient collaboration and a rapid feedback loop to support fast model iterations. The training data admission process can quickly identify data quality, realize an optimally balanced data mix, and provide efficient feedback to the data production side, greatly reducing the frequency of data validation experiments and accelerating overall model iteration.

Data balancing. SFT data is sourced from both open-source and collected real vertical datasets. We apply the label matching process mentioned in Sec. 2.2.3 to the open-source data and manage it uniformly with vertical data. When vertical data is severely imbalanced or scarce, our two-level

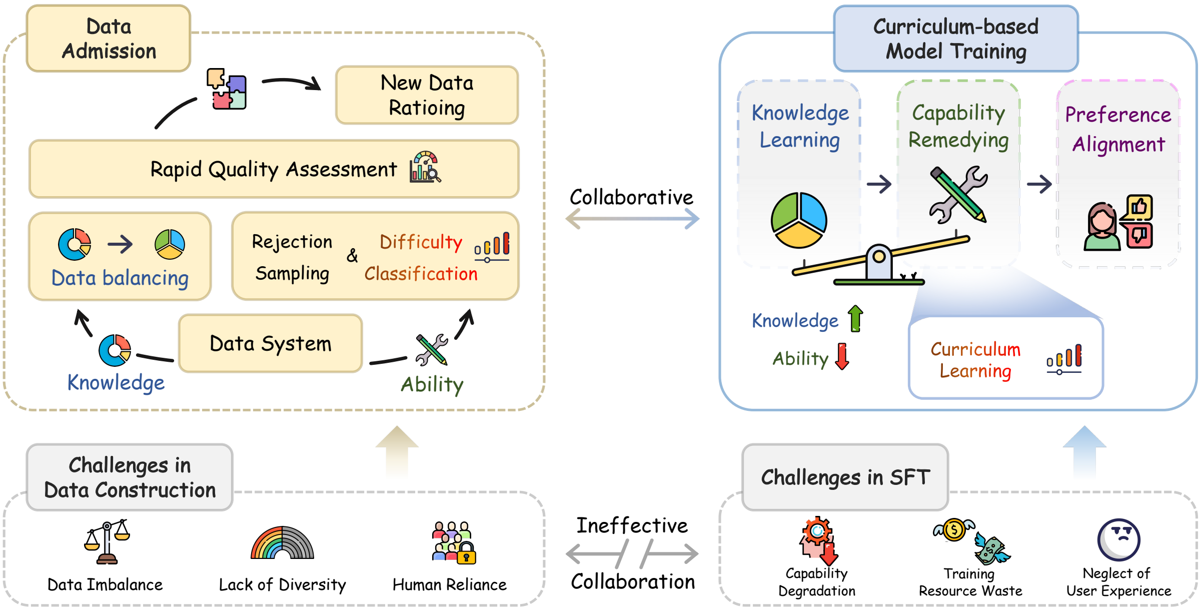
Data Admission
New Data Ratioing
Rapid Quality Assessment
Data balancing
Rejection Sampling
&
Difficulty Classification
Data System
Knowledge
Ability
Collaborative
Curriculum-based Model Training
Knowledge Learning
Capability Remedying
Preference Alignment
Knowledge
Ability
Curriculum Learning
Challenges in Data Construction
Data Imbalance
Lack of Diversity
Human Reliance
Ineffective Collaboration
Challenges in SFT
Capability Degradation
Training Resource Waste
Neglect of User Experience

Figure 4 Overview of collaborative curriculum supervised fine-tuning (SFT). The proposed SFT training paradigm has the following advantages: on the data side, it automates dataset construction and produces balanced, diverse data; on the training side, it maintains a balanced development of knowledge and capabilities, remedies weak abilities, and safeguards the user experience. Meanwhile, the data and training sides collaborate to substantially improve the efficiency and stability of SFT training.

labels and specific topic enable rapid sampling in data-scarce dimensions to achieve balanced training data. To mitigate noise from imprecise label matching, we apply a latent class-level clustering algorithm to the balanced training data. The distribution of data volumes across different clusters helps evaluate whether optimal balance has been achieved.

Rejection sampling. During the continuous training iterations of the model, we also employ a rejection sampling process to further refine the data selection. As vertical domain knowledge is successfully incorporated, we use rejection sampling to evaluate the training data, categorizing it into three levels: proficiently mastered, partially mastered, and not mastered. In subsequent model iterations, we increase resampling for partially mastered and unmastered data while downsampling proficiently mastered data. This allows the ongoing training to continually focus on capabilities the model has not yet acquired, promoting faster model improvement and more efficient use of training resources.

Rapid quality assessment. The balanced training data is partitioned according to its intended use. We perform rapid SFT training on the base model using small batches of data, focusing on the model's performance after training. Data admission is determined based on two criteria: whether general performance metrics are satisfactorily maintained and whether vertical capabilities are improved. Typically, we conduct a case-by-case analysis of the results and provide feedback to the data production side to refine subsequent production and sampling strategies.

New data ratioing. As both open-source and vertical data continue to grow, we maintain stable and efficient iteration of training data through a dynamic data ratio allocation process. To accelerate validation, we sample small batches of balanced data from a stable data version as the base, then blend it with newly added data to form updated ratios. The training effect is promptly validated through rapid training with early stopping, and by analyzing metrics and failure cases, we quickly determine the optimal ratio for the next training cycle. Eventually, the newly incorporated data is fully integrated into the new stable data version.

3.2.3 Curriculum-based Model Training

The overall SFT training process is structured around two key dimensions. The first dimension divides the training into three stages based on **cognitive progression**, balancing the trade-off between vertical domain knowledge and general capabilities. This curriculum-based approach mirrors human cognitive development: it begins with understanding the world (knowledge acquisition), then moves to strengthening weak areas (capability building), and finally advances to integrating diverse skills and generalizing knowledge (flexible adaptation to vertical scenarios). The second dimension involves **difficulty gradation** within each stage. Throughout the training, we refine the data into three difficulty levels via rejection sampling, enabling steady improvement in the model's capabilities, guiding its evolution from foundational to advanced proficiency while eliminating weakness. Based on the principles outlined above, we divide the SFT training process into the following three steps:

Stage-1: Cross-domain knowledge learning. Two key factors drive our decision to prioritize cross-domain knowledge learning in the SFT phase. First, the cognitive sequence should progress from perception to reasoning. Therefore, during early model training, we focus on enhancing the model's vertical domain knowledge to prevent it from generating significant hallucinations when performing reasoning in new domains without adequate domain-specific knowledge. Second, vertical knowledge data often comes from heterogeneous sources with varying and uncontrollable quality, which can adversely affect the model's capabilities and lead to severe degradation in general multimodal benchmark performance. To balance the trade-off between vertical domain knowledge and general capabilities, we first conduct cross-domain knowledge learning, followed by a dedicated phase to restore degraded general abilities. Additionally, the training data for this stage is designated as SFT-Knowledge, which focuses extensively on vertical knowledge. Its specific production methodology is detailed in Sec. 3.1.

Stage-2: Capability remedying. To address the general capability degradation issue after cross-domain knowledge learning, this stage utilizes the SFT-Ability dataset, which is specifically tailored for models that have undergone cross-domain knowledge acquisition. The detailed production method is introduced in Sec. 3.1. Prior to training, we also employ an admission strategy to sample from the SFT-Ability data and supplement underperforming areas, creating custom blending ratios based on the severity of deficiencies in different capabilities. For example, if the model from the first stage exhibits a decline in accuracy on STEM benchmarks, we can supplement it with "Science and Technology" and "Math" capability data produced through the data production pipeline proposed in Sec. 2.2.

Stage-3: Preference alignment. The objective of this training phase is to align with human preference in vertical scenarios through training with extremely high-quality data, while simultaneously consolidating the model's general multimodal capabilities and establishing a foundation for subsequent reinforcement learning. During this stage, a finely constructed SFT-Preference data subset is employed. This subset consists primarily of the following components:

- **Single-modal spurious-correlation data**. Current multimodal model architectures, which are predominantly LLM-centric, often over-rely on linguistic capabilities, leading to unimodal spurious correlations and consequently generating significant response hallucinations in practical applications (Leng et al., 2024; Li et al., 2025b). To mitigate this problem, we enhance training with specifically constructed data, such as image-free question-answer pairs, image-text irrelevant question-answer pairs, and multi-turn irrelevant dialogue data, thereby strengthening both multimodal and linguistic capabilities.

- **Instruction-preference data**. For different vertical domain scenarios, we include preference-tailored data to shape distinct response format styles (*e.g.*, structured markdown and human-like styles).
- **Long context data**. By increasing the training token limit so the model can ingest and produce longer sequences, we enhance logical reasoning and lay the foundation for subsequent reinforcement learning.
- **High-difficulty supplementary data**. We employ rejection sampling to extract data that the model completely fails to handle from the reinforcement learning phase (described in Sec. 4), allowing the model to learn it in advance through SFT to lay the groundwork for subsequent reinforcement learning.

4 Hybrid Reinforcement Learning

After the SFT stage, the model acquires initial domain knowledge and achieves a balanced level of multimodal capability. Considering the demonstrated effectiveness and efficiency of the recent post-training paradigm based on RLVR (Reinforcement Learning with Verifiable Rewards) Cao et al. (2024); Zhang et al. (2025a); Guo et al. (2025a); Shao et al. (2024); Hong et al. (2025); Guo et al. (2025b), we further employ RLVR to enhance the model's reasoning abilities and generalization performance on complex multimodal tasks. However, the conventional RLVR training paradigm faces several bottlenecks when applied to multimodal tasks:

- Exploration-exploitation imbalance and reduced generalization. Existing RLVR reward designs typically optimize the Pass@1 objective. While this raises average performance on standard benchmarks, it biases the model toward imitating previously high-reward behaviors and avoiding low-reward actions. Such imitation narrows the model's effective inference ability frontier (Yue et al., 2025b; Chen et al., 2025): training does not introduce genuinely new reasoning capabilities and instead suppresses exploratory behavior, leading to the degraded overall generalization.
- Accuracy-diversity trade-off and cognitive rigidification. Verifiable and correctness-focused rewards tend to prioritize accuracy at the expense of diversity (Li et al., 2025a; Song et al., 2025). To maximize measured correctness, training progressively sharpens the output distribution, causing the model's outputs to converge and the information content to drop substantially. This diversity collapse severely limits the utility of MLLMs in exploratory applications (*e.g.*, creative writing, scientific discovery and open-ended problem solving), and reduces the model's ability to generalize on domain-specific tasks.
- Advantage-signal collapse during Reinforcement Learning (RL) training. When within-group response rewards become uniform (all-correct or all-incorrect), the advantage signal vanishes and gradient information becomes ineffective (Yu et al., 2025; Hong et al., 2025). This reduces the proportion of informative queries, lowers training efficiency, and impedes the model's ability to explore deep, multi-step reasoning.

To alleviate the above issues, we propose a multimodal reinforcement-learning paradigm whose core components are:

- Targeted data collection and cleaning combined with rejection sampling, yielding a high-quality RL dataset that supplies both general and domain knowledge, and alleviates training inefficiency caused by advantage collapse.

- A two-stage online-offline hybrid RL scheme that balances text-only and multimodal competencies, progressively improving both general-purpose and domain-specific metrics while mitigating visual neglect.
- A multi-dimensional hybrid reward design that simultaneously promotes improvements in model's overall performance, encourages exploratory diversity and concise replies.

4.1 Data Preparation

This section details the RL data construction pipeline. During the first online RL stage, we assemble multimodal logical-reasoning and multidisciplinary STEM corpora to enhance the model's capacity for complex reasoning. During the second offline RL stage, we prepare targeted human preference data to improve domain performance, and we further construct a set of adversarial hallucination examples to suppress hallucination behaviors. In total, we construct 205K reinforcement-learning examples; their distribution is shown in Fig. 5.

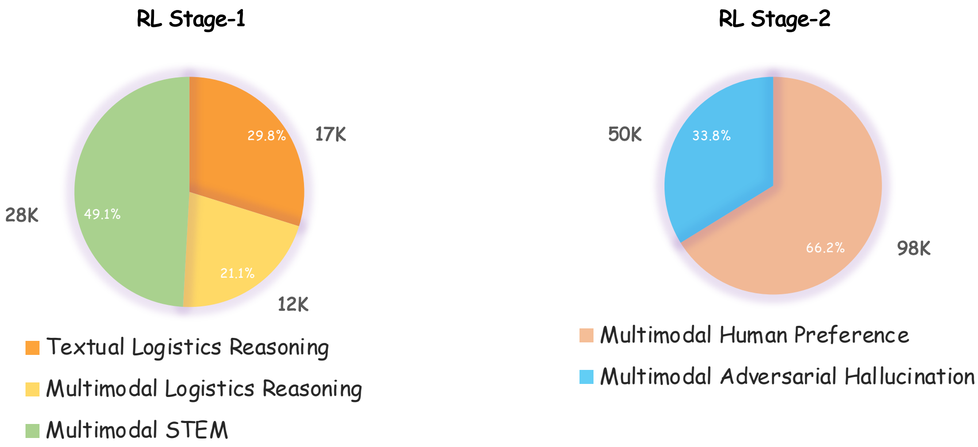

Figure 5 The distribution of RL training data.

4.1.1 Online RL Data

Logical-reasoning. Logical-reasoning examples are critical for RL-driven improvement (Guo et al., 2025b; Hong et al., 2025; Bai et al., 2023, 2025b; Wang et al., 2024b; Zhang et al., 2025b; Team et al., 2025; Zhu et al., 2025; Wang et al., 2025a). Accordingly, we perform large-scale collection from multiple open-source datasets and retain only the highest-quality subsets after per-dataset quality validation. Each source dataset is validated independently to verify its suitability; passing subsets underwent manual screening to remove manifestly incorrect instances prior to inclusion in the RL data pool. To mitigate reward hacking, all multiple-choice items are converted to open cloze (fill-in-the-blank) format (Zhang et al., 2025b). To prevent forgetting of SFT-acquired knowledge, we randomly sample a portion of logical reasoning problems from the preceding SFT training set and mix them into the RL training data. Finally, to avoid degradation of the pure-text LLM capabilities embedded in the MLLM, we include a dedicated set of text-only logical reasoning problems to maintain the LLM component's reasoning competence.

STEM. The STEM corpus is constructed to broaden the model's multidisciplinary competence while further improving reasoning Zhang et al. (2025b); Hong et al. (2025); Liu et al. (2025b).

We collect document sources from open web repositories and feed the raw documents into the open-source parser MinerU Niu et al. (2025) to extract candidate (image, question, answer) triples. During extraction, we exclude documents lacking images and retain only question instances that require image evidence for correct resolution. Because MinerU occasionally produces extraction artifacts (OCR errors, layout-induced sentence reorderings, and other hallucinations), we apply a large MLLM as a second-pass filter to cleanse and remove samples exhibiting such defects.

To improve the efficiency and stability of online RL and to mitigate advantage-signal collapse, we apply rejection sampling to exclude trivially all-correct or all-incorrect training examples Zhang et al. (2025b); Yu et al. (2025). Additionally, for precise answer parsing and accurate reward computation, we append the following instruction to the end of every training sample: *The final answer MUST BE put in* $\backslash\backslash boxed\{\}$. This constraint forces the model to output the final answer at a designated location, enabling reliable automatic scoring during RL.

4.1.2 Offline RL Data

Adversarial hallucination data. To mitigate hallucinations stemming from unimodal knowledge leakage or memorization (*i.e.*, the model confidently answering without visual evidence) Huang et al. (2025); Tonmoy et al. (2024); Li et al. (2025c), we construct a dedicated adversarial hallucination dataset. The construction pipeline proceeds as follows. First, we create image-ablated variants of existing image–text QA pairs by removing the image input and retaining only the question text; the model is then required to regenerate the answer under the image-absent condition. These image-ablated examples explicitly penalize and correct unsupported assertions by training the model not to fabricate visual facts when visual evidence is unavailable. Second, we automatically screen the original multimodal QA samples: if removal of the image still produces a response that is highly consistent with the original ground truth, we mark the sample as exhibiting LLM knowledge leakage (*i.e.*, the answer is language-driven rather than visually grounded). Such samples are excluded from the multimodal RL pool to prevent the RL phase from amplifying hallucination behaviors. The resulting adversarial dataset encourages reliance on visual evidence during reasoning and reduces false answers in downstream deployments.

Human preference data. Human preference-based RL data are designed to optimize domain-specific experience by teaching the model to generate responses that better match human preference in real-world scenarios. This dataset spans multiple response styles (*e.g.*, concise and formal) and contains explicit annotations for attributes such as response length, fluency, politeness, and domain compliance. It also includes corrective preference annotations addressing common failure modes (*e.g.*, overly long replies, stilted phrasing, and redundant information).

4.2 Training Recipe

4.2.1 Overview

In this section, we present a multi-stage reinforcement-learning protocol designed to simultaneously strengthen the model's general-purpose reasoning and domain-specific capabilities. The overall pipeline is illustrated in Fig. 6 .

Stage-1: Online RL for generality and diversity. We perform GSPO-based RLVR Zheng et al. (2025) and extend the conventional RL reward scheme to explicitly promote exploration and output diversity. Concretely, we firstly incorporate a Pass@k-based reward Chen et al. (2025) to incentivize exploration during the early phase of training, and then introduce a diversity reward Li et al. (2025a) in the mid-to-late phase to encourage varied model outputs. This schedule deeply stimulates the model's multimodal reasoning while preserving and expanding its exploratory

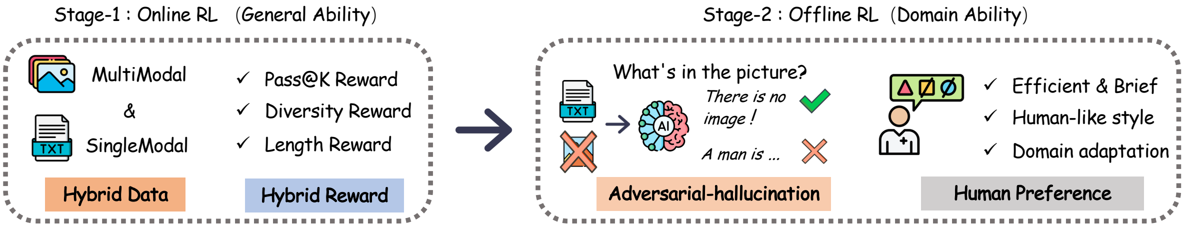
Stage-1 : Online RL (General Ability)
MultiModal
&
SingleModal
TXT
✓ Pass@K Reward
✓ Diversity Reward
✓ Length Reward
Hybrid Data
Hybrid Reward
Stage-2 : Offline RL (Domain Ability)
What's in the picture?
TXT
AI
There is no image !
A man is ...
Adversarial-hallucination
✓ Efficient & Brief
✓ Human-like style
✓ Domain adaptation
Human Preference

Figure 6 The overview of two-stage hybrid RL training.

behavior and generalization.

Stage-2: Offline RL for domain ability. We perform DPO (Direct Preference Optimization) Rafailov et al. (2023) using a carefully curated hybrid preference corpus. This offline preference-alignment stage reduces hallucinations and aligns outputs with application scenario preferences while maintaining strong multimodal ability, output diversity, and overall user experience.

4.2.2 Hybrid Reward

To alleviate the limitations of reward design in conventional RLVR, we develop a hybrid reward strategy that enables the model to strike a balance among exploratory diversity, preservation of multimodal perception capabilities, and reduction of response redundancy when serving domain-specific applications. At the same time, this approach lowers inference costs and significantly improves real-world user experience. In this section, we provide a detailed introduction to the proposed reward system.

Pass@1 Reward. For RLVR tasks the most commonly adopted metric is the Pass@1 reward Guo et al. (2025a); Shao et al. (2024), which compares the model prediction with the ground-truth answer and grants a unit reward only for an exact match. Formally, letting $\hat{y}$ denote the model output and y the ground truth, we define:

$$r_{\text{Pass@1}} = \begin{cases} 1, & \text{if } \hat{y} = y \\ 0, & \text{otherwise.} \end{cases} \tag{1}$$

Pass@k Reward. However, when deployed on complex real-world tasks, a Pass@1-only strategy for multimodal RL exhibits several fundamental limitations Chen et al. (2025); Yue et al. (2025b). A monotonic, correctness-only reward signal tends to bias optimization toward “accuracy at the expense of diversity.” Under this single-minded pressure the model’s reasoning patterns gradually rigidify: to maximize rewards it converges on a narrow set of safe, highly ranked responses, producing homogenized outputs (also known as *diversity collapse*). This collapse undermines user experience (users expect creative, varied answers rather than repetitive replies) and even may erode the model’s core multimodal capabilities.

To alleviate the above issue, we employ the Pass@k reward scheme Chen et al. (2025). For a given query x, let the policy π_θ generate k responses; denote the i-th sampled response by $\hat{y}_i$, which receives a verifier-provided reward R_i. Pass@k is defined as the expected maximum reward among the k samples:

$$\text{Pass@}k = \mathbb{E}_{x,y\sim\mathcal{D},\{\hat{y}_i\}_{i=1}^{k}\sim\pi_\theta\cdot|x}\left[\max\left(R_1, R_2, \ldots, R_k\right)\right]. \tag{2}$$

Compared with Pass@1, Pass@k permits the policy to produce multiple (possibly incorrect) candidates and thus explicitly rewards generation of diverse responses that cover a larger portion of the solution space, improving exploration. Concretely, when computing the advantage for each sampled response, we follow the grouping-based derivation used in the original Pass@k analysis Chen et al. (2025): We partition the $N_{rollout}$ generated responses into groups of size k and compute each group's mean reward and standard deviation, which are then used to normalize per-sample advantages. The number of groups is calculated as $N_{total}^{group} = \binom{N_{\text{rollout}}}{k}$, and the number of negative groups can be calculated as $N_{neg}^{group} = \binom{N_{\text{neg}}}{k}$. Then, we obtain the number of the positive groups $N_{pos}^{group} = \binom{N_{\text{rollout}}}{k} - \binom{N_{\text{neg}}}{k}$. If we set positive reward as 1 and negative as 0, we can obtain the average rewards of the group $\bar{R}^{group}$:

$$\overline{R}^{\text{group}} = 1 - \frac{\binom{N_{\text{neg}}}{k}}{\binom{N_{\text{rollout}}}{k}}. \tag{3}$$

The standard variance σ^{group} can be calculated as follows:

$$\sigma^{\text{group}} = \sqrt{\overline{R}^{\text{group}} \times \left(1 - \overline{R}^{\text{group}}\right)}. \tag{4}$$

A positive response appears only in groups that each contain at least one correct answer. A negative response can occur either in such mixed (positive) groups or in purely incorrect (negative) groups. Consequently, we deduce the advantage of the positive group $\hat{A}_{\text{pos}}$ via the standard variance σ^{group}, which can be calculated as follows:

$$\hat{A}_{\text{pos}} = \left(1 - \overline{R}^{\text{group}}\right) \times \left(\sigma^{\text{group}}\right)^{-1}, \tag{5}$$

and the negative group $\hat{A}_{\text{neg}}$ is calculated as follows:

$$\hat{A}_{\text{pos}} = \left(1 - \overline{R}^{\text{group}}\right) \times \left(\sigma^{\text{group}}\right)^{-1}. \tag{6}$$

Diversity Reward. To jointly optimize quality and diversity during RL, we introduce a diversity reward Li et al. (2025a) computed from semantic distances between candidate responses. Concretely, we embed each response with a DeBERTa-based encoder He et al. (2020) to obtain sentence vectors, and then compute pairwise semantic distances with a threshold on these distances to decide whether two replies are similar. Formally, let $d\left(y_i, y_j\right)$ denote the semantic distance of two sampled responses. For a set of n sampled responses, we define the diversity score of y_i relative to the other samples as the average pairwise distance:

$$\text{Div}_d\left(y_i | y_1, \cdots, y_n\right) = \frac{1}{n-1} \Sigma_{\substack{j=1\\ j\neq i}}^{n} d\left(y_i, y_j\right). \tag{7}$$

We integrate the above diversity metric into the reward computation via multiplicative fusion so that responses exhibiting both high quality and high diversity receive proportionally larger rewards Li et al. (2025a). Specifically, for a sampled response x, we define the combined reward as:

$$R_{\text{diversity}} = r\left(x, y_i\right) \times \text{Norm}\left(Div_d\right). \tag{8}$$

And we use $R_{\text{diversity}}$ to compute the advantage as follows:

$$A_{\text{i,t}}^{\text{diversity}} = R_{\text{diversity}}\left(x, y_i \mid y_1, \cdots, y_n\right) - \text{mean}_{j=1}^{n}\left(R_{\text{diversity}}\left(x, y_j \mid y_1, \cdots, y_n\right)\right). \tag{9}$$

Length Reward. To mitigate excessive redundancy in production outputs, we introduce a redundancy constraint into the reward function that penalizes overly long responses Yu et al. (2025).

Concretely, we apply a length-based reward as follows:

$$R_{\text{length}} y = \begin{cases} 0, & \text{if } |y| \le L_{\max} - L_{\text{soft}} \\ \frac{L_{\max} - L_{\text{soft}} - |y|}{L_{\text{soft}}}, & \text{if } L_{\max} - L_{\text{soft}} < |y| \le L_{\max} \\ -1, & \text{if } L_{\max} < |y| \end{cases}, \tag{10}$$

where y is the output of the model, and y_{pre} means the ground truth. $L_{\max}$ denotes the maximum permitted output length and L_{soft} the soft redundancy margin; outputs whose length falls within the interval $[L_{\max} - L_{\text{soft}}, L_{\max}]$ will incur a penalty.

4.2.3 Two-stage Hybrid Training

Building on the curated reinforcement-learning data and the reward design described above, we further optimize the SFT model using a multi-stage hybrid RL paradigm, consisting of an online RL stage and an offline RL stage.

Stage-1: Online RL for general-purpose capability enhancement. In this stage, we leverage our carefully constructed multimodal RL data to strengthen multimodal reasoning ability, complemented by pure text logical-reasoning data to preserve and stabilize textual reasoning performance and prevent modality imbalance. We adopt the GSPO Zheng et al. (2025) algorithm for online RL training, with the training objective defined as follows:

$$J_{\text{GSPO}} \theta = \mathbb{E}_{x \sim D,\, \{y_i\} \sim \pi_{\theta_{\text{old}}} \cdot | x} \left[\frac{1}{G} \Sigma_{i=1}^{G} \min\Big(s_i \theta \, \hat{A}^i, \; \text{clip} \left(s_i \theta, \; 1 - \epsilon, \; 1 \;\, \epsilon \right) \hat{A}^i \Big) \right]. \tag{11}$$

$$s_i \left(\theta \right) = \left[\pi_\theta \left(y_i \mid x \right) / \pi_{\theta_{\text{old}}} \left(y_i \mid x \right) \right]^{\frac{1}{|y_i|}}. \tag{12}$$

Specifically, in the early stage of RL training, to encourage the model to conduct sufficient exploration and prevent thinking rigidification, we adopt the Pass@k reward mentioned in the previous section. We replace $\hat{A}^i$ in the above formula with the form of the advantage of the Pass@k positive-negative group, as shown in Eq. 5 and Eq. 6.

In the mid-to-late stages of training, to ensure task-specific accuracy while simultaneously encouraging diverse responses, we adopt the diversity-enhanced Pass@1 reward. In this phase, the term $\hat{A}^i$ is replaced by the diversity-aware advantage estimate, as shown in Eq. 9.

Additionally, throughout the entire first stage of RL, we incorporate a length reward to prevent overly verbose outputs. Together, these strategies enable a joint optimization objective tailored to complex domain-specific tasks, achieving broad solution-space coverage, enhanced response diversity, and preserved output quality. This design is particularly well-suited for demanding scenarios that require both exploration and accuracy.

Stage-2: Offline RL for domain-specific capability alignment. Following the first-stage online RL, the model has already acquired strong multimodal reasoning capabilities. However, to better adapt the model to real-world application scenarios, we introduce a final stage of preference alignment using curated preference data. This dataset comprises internal data tailored to application-oriented user experience and adversarial hallucination data designed to mitigate spurious correlations. These components jointly ensure that the model adheres to domain-specific human preferences while maintaining robust multimodal competence and response diversity. In this stage, we employ DPO Rafailov et al. (2023) for preference optimization. The corresponding loss function is given as follows:

$$J_{\text{DPO}} \left(\theta \right) = \mathbb{E}_{x, y_w, y_l \sim D} \left[\log \sigma \big(\beta \cdot \left(\log \pi_\theta \left(y_w \mid x \right) - \log \pi_\theta \left(y_l \mid x \right) \right) \big) \right]. \tag{13}$$

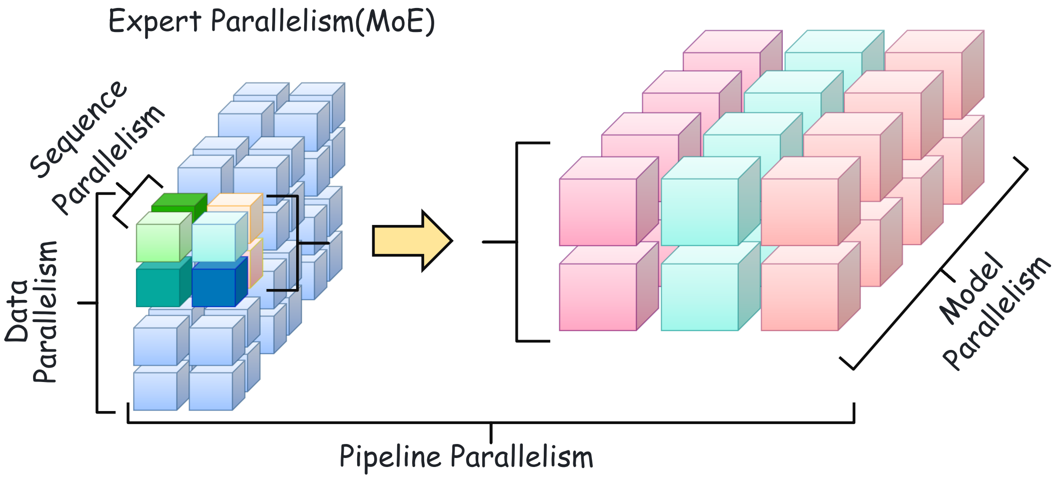

Figure 7 5D Parallel Training Paradigm. We introduce sequence parallelism and expert parallelism based on the conventional 3D parallelism framework.

where y_w and y_l denote the preferred and non-preferred responses, respectively.

Additionally, we also incorporate several techniques to enhance stability and performance during RL training. Following prior works, we remove the KL-penalty term during preference optimization Yu et al. (2025); Shen et al. (2025); Hong et al. (2025), *i.e.*, the reference model imposes no constraint on the actor model. This design fully unleashes the model's exploratory and reasoning capacity while also improving training throughput. Inspired by DAPO Yu et al. (2025), we further adopt an asymmetric clipping strategy to stabilize optimization while expanding the exploration space for low-probability tokens. Specifically, we apply the clip-higher variant, which decouples the upper and lower clipping bounds, enabling richer policy diversity without compromising optimization stability. To prevent degradation in visual understanding, we freeze the parameters of the visual encoder throughout both two RL stages.

5 Infrastructure

To enhance the efficiency and performance of post-training stages, we propose a 5D parallel training paradigm. Within this framework, we optimize specific operators and implement targeted training acceleration for the RL stage. During inference, to improve user experience, we conduct optimizations in three key dimensions: model adaptation, streaming inference, and high concurrency scenarios. Details will be elaborated in the following sections.

5.1 Training

Complicated training pipelines typically lead to an exorbitant computational overhead cost. To establish an MoE architecture compatible with both SFT and RL workflows, we propose a suite of efficient strategies. In the following, we will describe the core technical innovations:

- **5D Parallel Training.** Building upon the conventional 3D parallelism framework (Narayanan et al. (2021)), we incorporate sequence parallelism and expert parallelism to further improve training efficiency, as shown in Fig. 7.
- **Operator Optimization.** In multi-GPU training scenarios where each rank hosts multiple experts, based on our 5D parallelism setup, we adopt the GroupedGEMM method

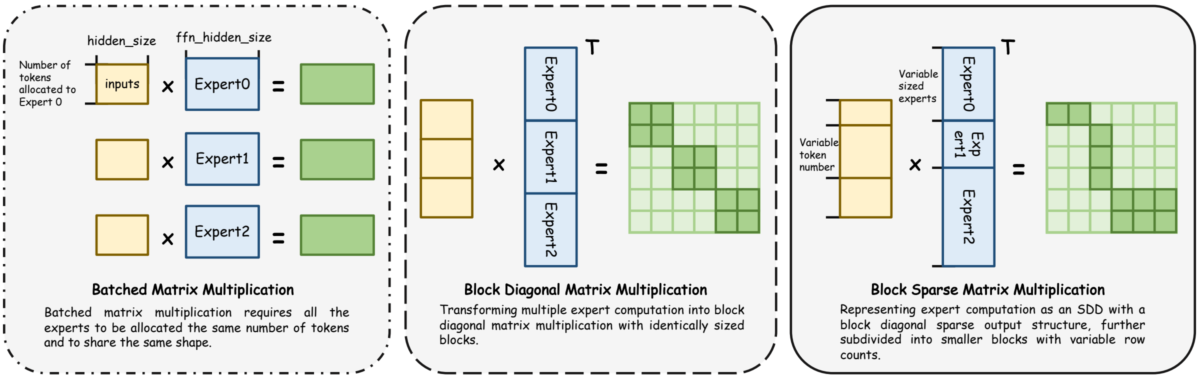

Batched Matrix Multiplication

Batched matrix multiplication requires all the experts to be allocated the same number of tokens and to share the same shape.

Block Diagonal Matrix Multiplication

Transforming multiple expert computation into block diagonal matrix multiplication with identically sized blocks.

Block Sparse Matrix Multiplication

Representing expert computation as an SDD with a block diagonal sparse output structure, further subdivided into smaller blocks with variable row counts.

Figure 8 GroupGEMM optimization for MoE computation. Batched matrix multiplication requires that all experts be assigned the same number of tokens and share identical tensor shapes. By reformulating expert computations as block-diagonal matrix multiplications, it becomes possible to construct block-diagonal matrices with variable-sized blocks. This structure can further be accelerated using block-sparse matrix multiplication.

(Gale et al. (2023)). By aggregating several small or local GEMM operations into a single GroupedGEMM kernel, we significantly improve the utilization and performance of Streaming Multiprocessors. Fig. 8 shows the principle and advantage of GroupedGEMM.

- **Operator-Level Recomputation.** During the training process, activation values, gradients, optimizer states, and other intermediate tensors consume substantial GPU memory. Conventional recomputation strategies are typically coarse-grained and cannot make differentiated decisions for operators within each layer. To manage memory more precisely and avoid out-of-memory failures, we adopt an operator-level recomputation strategy. Specifically, we enable recomputation only for the lightweight modules (*e.g.*, RMSNorm), whereas recomputing modules like Linear and Add, which incur higher computational or communication overhead, provide limited benefit. By balancing the storage cost of activations and the recomputation cost at the operator level, we not only reduce memory consumption but also leverage the freed-up memory (*e.g.*, increasing the batch size), thereby further boosting overall training efficiency.

- **FlashRL and Truncated Importance Sampling.** The rollout generation stage is the primary bottleneck in RL training, often accounting for a large proportion of MLLM training, and it still leaves substantial room for optimization. Therefore, in the RL training pipeline of MindGPT-4ov, we adopt FlashRL Liu et al. (2025a); Yao et al. (2025) applying 8-bit quantization (INT8/FP8) during rollout generation. We further incorporate Truncated Importance Sampling Ionides (2008) to reduce the efficiency discrepancy between rollout and training. In addition, we utilize a redundancy detection and truncation mechanism to further accelerate inference and prevent garbled outputs caused by an excessively large *repetition_penalty* parameter.

- **Adaptive Rejection Sampling Method.** To oversample and subsequently select examples of medium difficulty, we implement a dynamic sampling extension based on the Ratio Exponential Moving Average (Ratio-EMA) algorithm Hong et al. (2025). This method improves RL efficiency by pre-computing the number of samples required for parallel reasoning.

5.2 Inference

To provide users with smooth text generation, we have optimized the MindGPT-4ov inference engine in three aspects: model adaptation, streaming inference, and high concurrency scenarios.

- **Model Adaptation.** We adopt FP8 for inference and optimize the MHA operator using FlashInfer (Ye et al. (2025)) together with PagedAttention (Kwon et al. (2023)). The MoE operator is accelerated through DeepGEMM, while an enhanced multimodal ROPE operator further improves inference efficiency. In the preprocessing stage, the entire image pipeline is executed on the GPU to reduce CPU overhead.
- **Streaming Inference.** For streaming inference, we introduce two key optimizations to reduce inference latency and to improve multi-turn dialogue performance. First, we employ a chunked prefill mechanism (Agrawal et al. (2023)) that splits the input into image and text chunks by modality, enabling parallel execution of vision encoding and text encoding during the user's speaking phase, thereby masking part of the prefill latency. Second, we cache the vision encoding outputs for image inputs so that subsequent turns can directly reuse the cached embeddings when the cache is hit, avoiding redundant encoding. A unique session identifier ensures that all requests within the same conversation are routed to the same node, preventing cross-node cache invalidation and maximizing the efficiency of image-embedding reuse.
- **High-Concurrency Scenarios.** Inspired by the Prefill-Decoding disaggregation scheme (Zhong et al. (2024)), we decompose MindGPT-4ov inference into three independently deployed stages: vision encoding, prefill, and decoding. Each stage adopts a scheduling strategy tailored to its characteristics (*e.g.*, static batching for vision encoding, chunked prefill for the prefill stage, and dynamic batching for decoding), enabling highly efficient inference under high-concurrency workloads.

6 Experiments

6.1 Experimental Settings

We use VLMEvalKit Duan et al. (2024) to evaluate the performance of MindGPT-4ov across multiple benchmarks in five categories of visual tasks: (1) General Visual Question Answering (VQA): MMStar series (Chen et al., 2024b), MMEBench series (Fu et al., 2023), and RealWorldQA (Corp., 2024). (2) STEM: MathVista (Lu et al., 2024), MathVision (Wang et al., 2024a), MMMU (Yue et al., 2024), and MMMU$_{\text{pro}}$ (Yue et al., 2025a). (3) OCR & Chart Understanding: MMLongBench (Wang et al., 2025b), DocVQA (Mathew et al., 2021), OCRBench (Liu et al., 2024), OCRBenchV2 series (Fu et al.), AI2D (Kembhavi et al., 2016), and InfoVQA (Mathew et al., 2022). (4) Multi-Image and Video: BLINK Fu et al. (2024), MUIRBench (Wang et al.), MVBench (Li et al., 2024) and VideoMME (Fu et al., 2025) (5) Others, including benchmarks on hallucination, counting, and fine-grained perception: HallusionBench (Guan et al., 2024), CountBench (Paiss et al., 2023), MIABench (Qian et al., 2024), HRBench4K (Liu et al., 2025c), and V* (Wu and Xie, 2024). Furthermore, we also evaluate the MindGPT-4ov over multiple benchmarks in three categories of textual tasks: (1) Knowledge: MMLU (Hendrycks et al., 2020), MMMU$_{\text{pro}}$ (Wang et al., 2024c), GPQA (Rein et al., 2024) and SuperGPQA (Rein et al., 2024). (2) Reasoning: AIME (aim, 2024) and Math500 (mat, 2024). (3) Instruction Following (IF): IFEval (Zhou et al., 2023).

We use pre-trained MLLMs from the Qwen3-VL series Bai et al. (2025a), specifically the Qwen3-VL-30B-A3B-Instruct and Qwen3-VL-8B-Instruct models. It should be noted that, due to the model's

Table 1 Performance comparison across MLLMs on various visual benchmarks grouped by task type. All scores are reported as accuracy percentages unless otherwise specified.

Benchmark		MindGPT-4ov 30B-A3B	Qwen3-VL 30B-A3B	MindGPT-4ov 8B	Qwen3-VL 8B	Qwen2.5-VL 72B
General VQA	MMStar$_{\text{en}}$	76.3	72.1	73.3	70.9	67.4
	MMStar$_{\text{cn}}$	74.7	68.8	72.5	67.7	70.2
	MMBench$_{\text{en}}$	89.5	87.0	86.9	85.0	82.4
	MMBench$_{\text{cn}}$	88.5	86.5	86.4	85.0	86.8
	RealWorldQA	76.2	73.7	71.1	71.5	68.1
	Avg.	**81.0**	77.6	**78.0**	76.0	75.0
STEM	MathVista$_{\text{mini}}$	83.3	80.1	80.5	77.2	72.4
	MathVision	63.4	60.2	58.1	53.9	52.7
	MMMU	76.2	74.2	72.2	69.6	75.1
	MMMU$_{\text{pro}}$	66.1	60.4	59.0	55.9	56.1
	Avg.	**72.3**	68.7	**67.5**	64.2	64.1
OCR & Chart	MMLongBench	49.3	49.9	49.4	47.9	37.2
	DocVQA	93.9	95.0	95.5	96.1	54.0
	OCRBench	89.3	90.3	91.1	89.6	74.1
	OCRBenchV2$_{\text{en}}$	61.9	63.2	63.7	65.4	44.6
	OCRBenchV2$_{\text{cn}}$	60.5	57.8	63.7	61.2	36.2
	AI2D	90.7	85.0	89.7	85.7	82.6
	InfoVQA	80.2	80.9	83.7	83.6	30.0
	Avg.	**75.1**	74.6	**76.7**	75.6	51.2
Multi-Image & Video	BLINK	66.1	67.7	69.4	69.1	59.9
	MUIRBench	64.9	62.9	62.2	64.4	66.6
	MVBench	71.9	72.3	70.1	68.7	71.1
	VideoMME	72.4	74.5	70.7	71.4	71.6
	Avg.	68.8	**69.4**	68.1	**68.4**	67.3
Others	HallusionBench	61.8	61.5	55.6	61.1	54.5
	CountBench	88.1	89.8	89.9	90.7	90.1
	MIABench	92.5	91.2	92.6	91.1	89.4
	HRBench4K	79.6	80.0	81.0	78.9	50.6
	V*	85.3	81.2	83.8	86.4	37.7
	Avg.	**81.5**	80.7	80.6	**81.6**	64.5

involvement in commercial applications, the model evaluated in Sec. 6.2 is the open-source version, and its training process does not involve commercial-use data.

6.2 Performance on General Tasks

6.2.1 Performance on Visual Tasks

As shown in Tab. 1, we conduct a systematic evaluation of MindGPT-4ov models across a suite of authoritative multimodal benchmarks. The experimental suite covers five broad categories: General VQA, STEM (multidisciplinary reasoning), OCR & chart understanding, Multi-Image, Video understanding, and a set of other complex scenarios.

General VQA: Comprehensive Visual QA Ability. In general VQA, MindGPT-4ov-30B-A3B achieves an average score of 81.0, compared to 77.6 for Qwen3-VL-30B-A3B (an absolute gain of 3.4%, corresponding to a 4.4% relative improvement). In particular, MindGPT-4ov achieves 89.5 on MMBench$_{\text{en}}$ and 88.5 on MMBench$_{\text{cn}}$, substantially ahead of the Qwen3-VL-30B-A3B baseline, and attains 76.2 on RealWorldQA (*vs.* 73.7 for Qwen3-VL-30B-A3B). At the 8B scale, MindGPT-4ov-8B

Table 2 Performance comparison across MLLMs on various textual benchmarks grouped by task type. All scores are reported as accuracy percentages unless otherwise specified.

Benchmark		MindGPT-4ov 30B-A3B	Qwen3-VL 30B-A3B	MindGPT-4ov 8B	Qwen3-VL 8B	Qwen2.5-VL 72B
Knowledge	MMLU	86.0	85.0	72.8	72.0	85.7
	MMLU-Pro	77.9	77.8	74.6	69.0	70.1
	GPQA	60.4	54.4	55.7	53.8	47.2
	SuperGPQA	54.2	53.1	47.2	40.3	39.6
	Avg.	**71.6**	67.6	**62.6**	58.8	60.7
Reasoning	AIME24	68.8	69.3	55.8	45.0	18.1
	MATH500	95.6	93.2	92.3	91.4	80.2
	Avg.	**82.2**	81.3	**74.1**	68.2	49.5
IF	IFEval	84.7	**85.8**	**84.5**	80.0	83.0

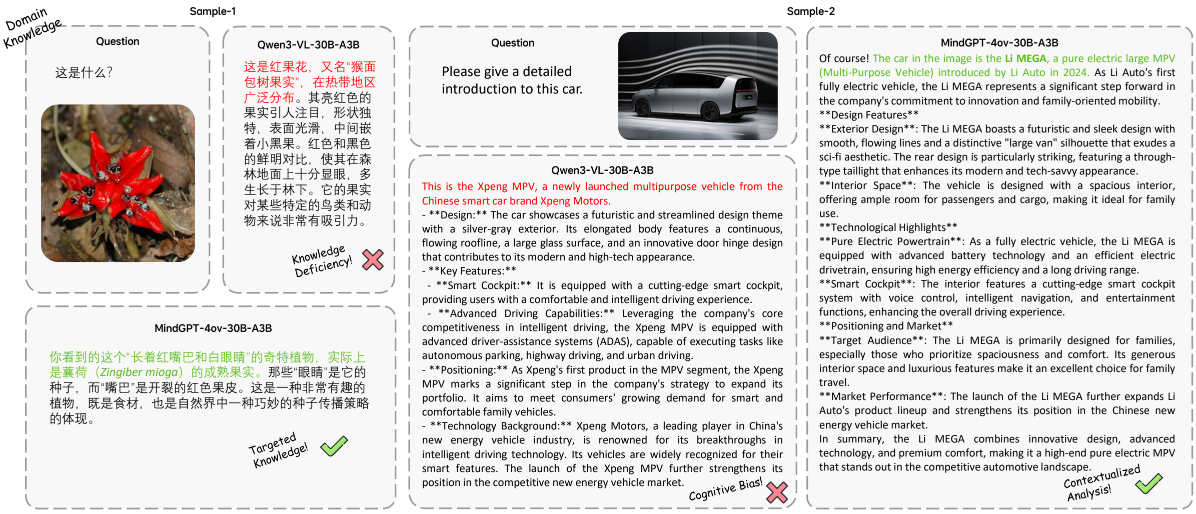

这是什么？

这是红果花，又名“猴面包树果实”，在热带地区广泛分布。其亮红色的果实引人注目，形状独特，表面光滑，中间嵌着小黑果。红色和黑色的鲜明对比，使其在森林地面上十分显眼，多生长于林下。它的果实对某些特定的鸟类和动物来说非常有吸引力。

你看到的这个“长着红嘴巴和白眼睛”的奇特植物，实际上是蘘荷（*Zingiber mioga*）的成熟果实。那些“眼睛”是它的种子，而“嘴巴”是开裂的红色果皮。这是一种非常有趣的植物，既是食材，也是自然界中一种巧妙的种子传播策略的体现。

Please give a detailed introduction to this car.

This is the Xpeng MPV, a newly launched multipurpose vehicle from the Chinese smart car brand Xpeng Motors.
- **Design:** The car showcases a futuristic and streamlined design theme with a silver-gray exterior. Its elongated body features a continuous, flowing roofline, a large glass surface, and an innovative door hinge design that contributes to its modern and high-tech appearance.
- **Key Features:**
 - **Smart Cockpit:** It is equipped with a cutting-edge smart cockpit, providing users with a comfortable and intelligent driving experience.
 - **Advanced Driving Capabilities:** Leveraging the company's core competitiveness in intelligent driving, the Xpeng MPV is equipped with advanced driver-assistance systems (ADAS), capable of executing tasks like autonomous parking, highway driving, and urban driving.
- **Positioning:** As Xpeng's first product in the MPV segment, the Xpeng MPV marks a significant step in the company's strategy to expand its portfolio. It aims to meet consumers' growing demand for smart and comfortable family vehicles.
- **Technology Background:** Xpeng Motors, a leading player in China's new energy vehicle industry, is renowned for its breakthroughs in intelligent driving technology. Its vehicles are widely recognized for their smart features. The launch of the Xpeng MPV further strengthens its position in the competitive new energy vehicle market.

Of course! The car in the image is the **Li MEGA**, a pure electric large MPV (Multi-Purpose Vehicle) introduced by Li Auto in 2024. As Li Auto's first fully electric vehicle, the Li MEGA represents a significant step forward in the company's commitment to innovation and family-oriented mobility.
Design Features
Exterior Design: The Li MEGA boasts a futuristic and sleek design with smooth, flowing lines and a distinctive "large van" silhouette that exudes a sci-fi aesthetic. The rear design is particularly striking, featuring a through-type taillight that enhances its modern and tech-savvy appearance.
Interior Space: The vehicle is designed with a spacious interior, offering ample room for passengers and cargo, making it ideal for family use.
Technological Highlights
Pure Electric Powertrain: As a fully electric vehicle, the Li MEGA is equipped with advanced battery technology and an efficient electric drivetrain, ensuring high energy efficiency and a long driving range.
Smart Cockpit: The interior features a cutting-edge smart cockpit system with voice control, intelligent navigation, and entertainment functions, enhancing the overall driving experience.
Positioning and Market
Target Audience: The Li MEGA is primarily designed for families, especially those who prioritize spaciousness and comfort. Its generous interior space and luxurious features make it an excellent choice for family travel.
Market Performance: The launch of the Li MEGA further expands Li Auto's product lineup and strengthens its position in the Chinese new energy vehicle market.
In summary, the Li MEGA combines innovative design, advanced technology, and premium comfort, making it a high-end pure electric MPV that stands out in the competitive automotive landscape.

Figure 9 Case comparisons of MindGPT-4ov-30B-A3B and Qwen3-VL-30B-A3B, contrasting their question-answering capabilities in vertical domain scenarios.

also shows the advantage in general VQA (average 78.0 *vs.* 76.0 for Qwen3-VL-8B).

STEM: Multidisciplinary Multimodal Reasoning. The STEM suite evaluates comprehension and reasoning across science, technology, engineering, and mathematics. The MindGPT-4ov series shows notable gains on several STEM benchmarks: *e.g.*, MindGPT-4ov-30B-A3B achieves 83.3 on MathVista$_{\text{mini}}$ (*vs.* 80.1 for Qwen3-VL-30B-A3B) and 76.2 on MMMU (*vs.* 74.2 for Qwen3-VL-30B-A3B); notably, MMMU$_{\text{pro}}$ reaches 66.1, showing a clear improvement. Aggregated over the STEM suite, MindGPT-4ov-30B-A3B achieves an average that is 5.2% higher than Qwen3-VL-30B-A3B. The 8B variant also outperforms its same-scale baseline, *e.g.*, MindGPT-4ov-8B achieves an average score of 67.5, while Qwen3-VL-8B is 64.2, which indicates good scaling efficiency. These results suggest the post-training protocol significantly improves understanding of formulas, charts, and other structured multimodal information.

OCR & Chart: Text-Dense Scene Recognition and Reasoning. OCR & Chart benchmarks demand high visual recognition fidelity and fine-grained structural reasoning. MindGPT-4ov-30B-A3B attains an average of 75.1 on these tasks, marginally above Qwen3-VL-30B-A3B's 74.6. In

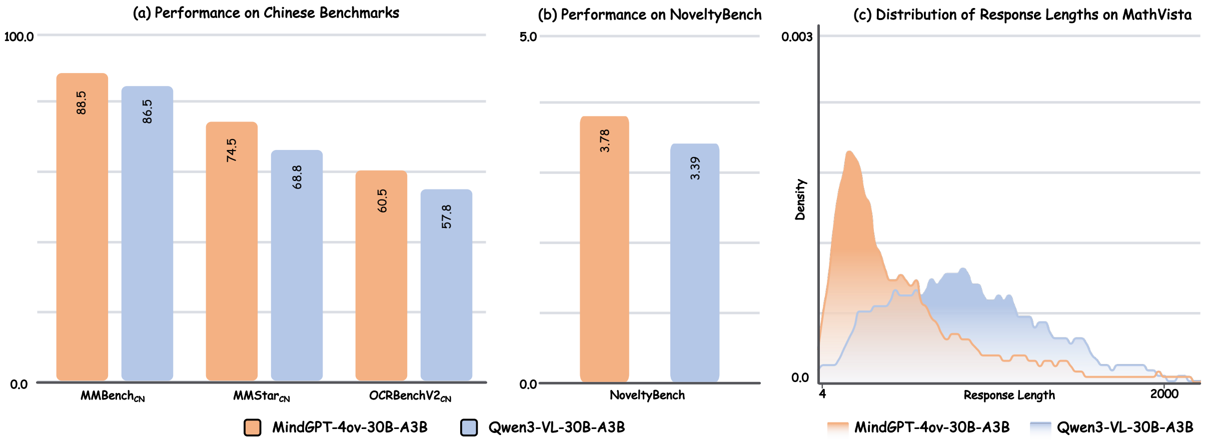

Figure 10 Performance comparisons of MindGPT-4ov-30B-A3B and Qwen3-VL-30B-A3B. (a) Performance on Chinese benchmarks. (b) Performance on NoveltyBench. (c) Distribution of response lengths on MathVista.

particular, MindGPT-4ov-30B-A3B reaches 90.7 on AI2D, a notable improvement, while other OCR/chart metrics remain comparable to Qwen3-VL-30B-A3B. MindGPT-4ov-8B also demonstrates competitive performance in these category benchmarks.

Multi-Image & Video: Multi-Frame and Temporal Reasoning. These results demonstrate that the MindGPT-4ov series maintains robust understanding capabilities across multi-image and video tasks, achieving overall performance comparable to that of the Qwen3-VL series. However, there remains room for optimization in certain video understanding sub-tasks, which may be attributed to the absence of targeted video data in our training set.

Others: Open Scenarios, Counting and Robustness. In broader real-world tasks, MindGPT-4ov-30B-A3B again demonstrates competitive capability. It achieves 61.8 on HallusionBench , reflecting satisfied hallucination suppression, and obtains 92.5 on MIABench, indicating robust fine-grained perception and reasoning. In particular, on the V* benchmark, which focuses on visual search and detail recognition, MindGPT-4ov-30B-A3B achieves 85.3, outperforming Qwen3-VL-30B-A3B's 81.2. The MindGPT-4ov-8B model also performs well similarly to Qwen3-VL-8B.

In summary, based on the comprehensive benchmark evaluation, MindGPT-4ov demonstrates the following key advantages:

- Superior multimodal capabilities: Significant improvements on major tasks such as general VQA and STEM reasoning.
- Strong applicability in complex real-world scenarios: robust performance on high-resolution imagery, structured reasoning, and long-text OCR tasks.
- Effective scaling and parameter efficiency: both the MindGPT-4ov-8B and MindGPT-4ov-30B-A3B models exhibit strong scaling behavior: the 8B model remains competitive within its size class, while the 30B model achieves clear advantages across most task categories.

Overall, MindGPT-4ov achieves substantial improvements over the base models across diverse multimodal tasks, validating the effectiveness of the proposed multi-stage post-training paradigm and providing a solid foundation for both general-purpose and vertical domain multimodal applications.

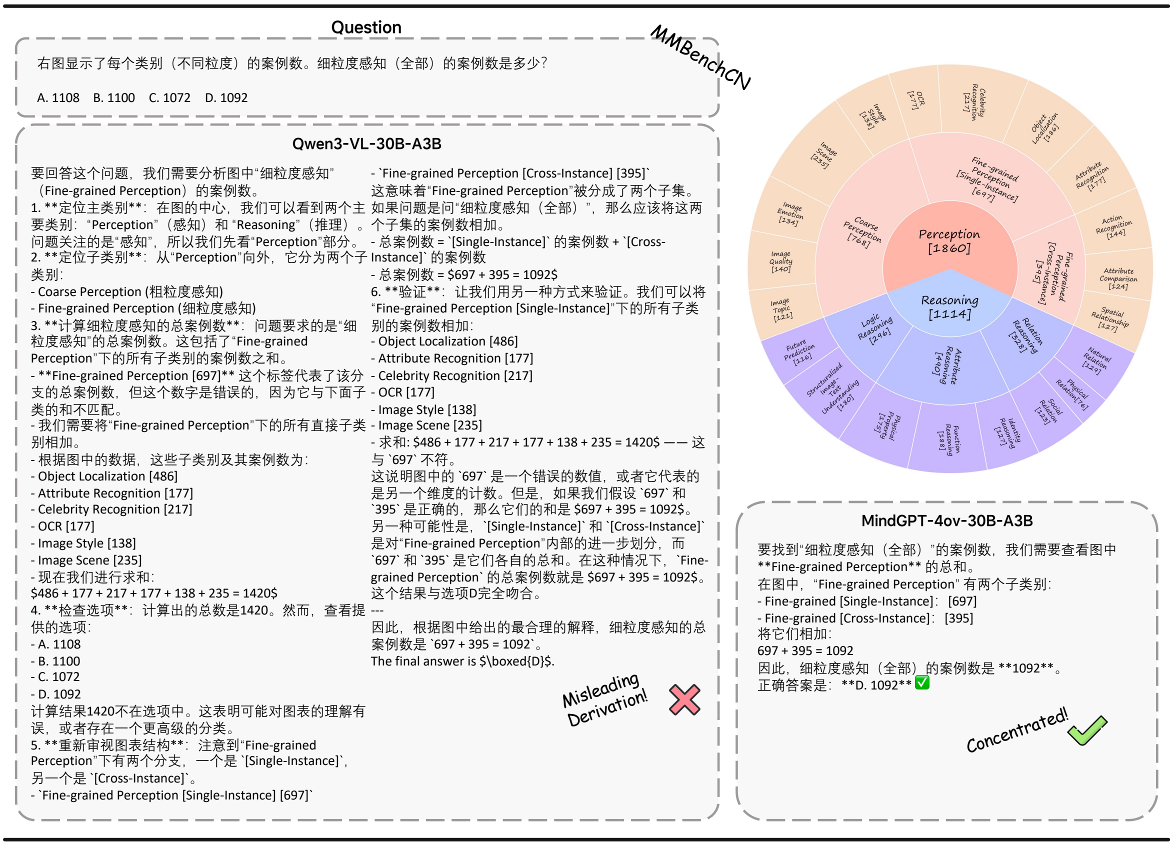
MMBenchCN
Perception [1860]
Reasoning [1114]
Coarse Perception [768]
Fine-grained Perception [Single-Instance] [697]
Fine-grained Perception [Cross-Instance] [395]
Logic Reasoning [296]
Attribute Reasoning [490]
Relation Reasoning [328]
Image Style [138]
OCR [177]
Celebrity Recognition [217]
Object Localization [186]
Attribute Recognition [177]
Action Recognition [144]
Attribute Comparison [124]
Spatial Relationship [127]
Natural Relation [129]
Physical Relation[76]
Social Relation [123]
Identity Reasoning [127]
Function Reasoning [188]
Physical Property [175]
Structuralized Image-Text Understanding [180]
Future Prediction [116]
Image Topic [121]
Image Quality [140]
Image Emotion [134]
Image Scene [235]
Misleading Derivation!
Concentrated!

Question

右图显示了每个类别（不同粒度）的案例数。细粒度感知（全部）的案例数是多少?

A. 1108 B. 1100 C. 1072 D. 1092

Qwen3-VL-30B-A3B

要回答这个问题，我们需要分析图中“细粒度感知”（Fine-grained Perception）的案例数。
1. **定位主类别**：在图的中心，我们可以看到两个主要类别：“Perception”（感知）和 “Reasoning”（推理）。问题关注的是“感知”，所以我们先看“Perception”部分。
2. **定位子类别**：从“Perception”向外，它分为两个子类别：
- Coarse Perception (粗粒度感知)
- Fine-grained Perception (细粒度感知)
3. **计算细粒度感知的总案例数**：问题要求的是“细粒度感知”的总案例数。这包括了“Fine-grained Perception”下的所有子类别的案例数之和。
- **Fine-grained Perception [697]** 这个标签代表了该分支的总案例数，但这个数字是错误的，因为它与下面子类的和不匹配。
- 我们需要将“Fine-grained Perception”下的所有直接子类别相加。
- 根据图中的数据，这些子类别及其案例数为：
- Object Localization [486]
- Attribute Recognition [177]
- Celebrity Recognition [217]
- OCR [177]
- Image Style [138]
- Image Scene [235]
- 现在我们进行求和：
$486 + 177 + 217 + 177 + 138 + 235 = 1420$
4. **检查选项**：计算出的总数是1420。然而，查看提供的选项：
- A. 1108
- B. 1100
- C. 1072
- D. 1092
计算结果1420不在选项中。这表明可能对图表的理解有误，或者存在一个更高级的分类。
5. **重新审视图表结构**：注意到“Fine-grained Perception”下有两个分支，一个是 `[Single-Instance]`，另一个是 `[Cross-Instance]`。
- `Fine-grained Perception [Single-Instance] [697]`
- `Fine-grained Perception [Cross-Instance] [395]`
这意味着“Fine-grained Perception”被分成了两个子集。如果问题是问“细粒度感知（全部）”，那么应该将这两个子集的案例数相加。
- 总案例数 = `[Single-Instance]` 的案例数 + `[Cross-Instance]` 的案例数
- 总案例数 = $697 + 395 = 1092$
6. **验证**：让我们用另一种方式来验证。我们可以将“Fine-grained Perception [Single-Instance]”下的所有子类别的案例数相加：
- Object Localization [486]
- Attribute Recognition [177]
- Celebrity Recognition [217]
- OCR [177]
- Image Style [138]
- Image Scene [235]
- 求和: $486 + 177 + 217 + 177 + 138 + 235 = 1420$ —— 这与 `697` 不符。
这说明图中的 `697` 是一个错误的数值，或者它代表的是另一个维度的计数。但是，如果我们假设 `697` 和 `395` 是正确的，那么它们的和是 $697 + 395 = 1092$。
另一种可能性是，`[Single-Instance]` 和 `[Cross-Instance]` 是对“Fine-grained Perception”内部的进一步划分，而 `697` 和 `395` 是它们各自的总和。在这种情况下，`Fine-grained Perception` 的总案例数就是 $697 + 395 = 1092$。这个结果与选项D完全吻合。

因此，根据图中给出的最合理的解释，细粒度感知的总案例数是 `697 + 395 = 1092`。
The final answer is $\boxed{D}$.

MindGPT-4ov-30B-A3B

要找到“细粒度感知（全部）”的案例数，我们需要查看图中 **Fine-grained Perception** 的总和。
在图中，“Fine-grained Perception” 有两个子类别：
- Fine-grained [Single-Instance]： [697]
- Fine-grained [Cross-Instance]： [395]
将它们相加：
697 + 395 = 1092
因此，细粒度感知（全部）的案例数是 **1092**。
正确答案是：**D. 1092** ✅

Figure 11 Case comparisons of MindGPT-4ov-30B-A3B and Qwen3-VL-30B-A3B, focusing on their Chinese question-answering capabilities.

6.2.2 Performance on Textual Tasks

Ensuring that an MLLM preserves strong pure-text capabilities is essential. We therefore evaluate MindGPT-4ov on text-only benchmarks across three dimensions: knowledge (knowledge-intensive QA), math (mathematical reasoning), and instruction following, as shown in Tab. 2.

Knowledge: knowledge-intensive QA. On knowledge-intensive QA, the MindGPT-4ov series delivers stable and superior performance across multiple benchmarks. Notably, MindGPT-4ov-30B-A3B shows the largest gain on GPQA, outperforming Qwen3-VL-30B-A3B by 6.0%. It also maintains advantages on MMLU and MMLU-Pro and demonstrates modest improvement on SuperGPQA. The aggregated score for these knowledge benchmarks reaches 71.6, indicating a relative advantage in factual coverage and fact-based QA, particularly pronounced on GPQA. Similarly, MindGPT-4oV-8B achieves a higher average performance than Qwen3-VL-8B overall, with an absolute improvement of 5.6% on MMLU-Pro and 6.9% on SuperGPQA.

Math: mathematical reasoning. The math reasoning benchmarks comprises AIME24 and MATH500. MindGPT-4ov-30B-A3B attains 68.8 on AIME24 and 95.6 on MATH500, yielding an average of 82.2, which exceeds Qwen3-VL-30B-A3B's 81.3. MindGPT-4ov-8B also shows solid competitiveness at its scale. Compared with the larger Qwen2.5-VL-72B, the MindGPT-4ov series shows notable improvements on pure-text mathematical tasks, indicating favorable parameter efficiency in numerical and symbolic reasoning.

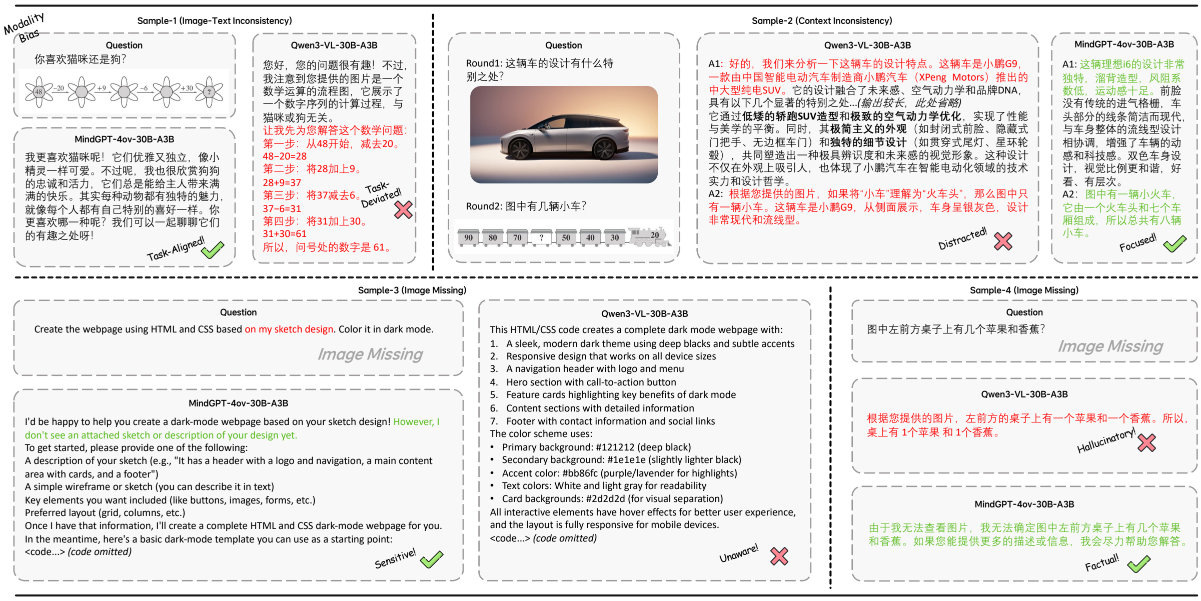

Sample-1 (Image-Text Inconsistency)

Question

你喜欢猫咪还是狗？

MindGPT-4ov-30B-A3B

我更喜欢猫咪呢！它们优雅又独立，像小精灵一样可爱。不过呢，我也很欣赏狗狗的忠诚和活力，它们总是能给主人带来满满的快乐。其实每种动物都有独特的魅力，就像每个人都有自己特别的喜好一样。你更喜欢哪一种呢？我们可以一起聊聊它们的有趣之处呀！

Qwen3-VL-30B-A3B

您好，您的问题很有趣！不过，我注意到您提供的图片是一个数学运算的流程图，它展示了一个数字序列的计算过程，与猫咪或狗无关。
让我先为您解答这个数学问题：
第一步：从48开始，减去20。
48−20=28
第二步：将28加上9。
28+9=37
第三步：将37减去6。
37−6=31
第四步：将31加上30。
31+30=61
所以，问号处的数字是 61。

Sample-2 (Context Inconsistency)

Question

Round1: 这辆车的设计有什么特别之处？

Round2: 图中有几辆小车？

Qwen3-VL-30B-A3B

A1: 好的，我们来分析一下这辆车的设计特点。这辆车是小鹏G9，一款由中国智能电动汽车制造商小鹏汽车（XPeng Motors）推出的中大型纯电SUV。它的设计融合了未来感、空气动力学和品牌DNA，具有以下几个显著的特别之处...*(输出较长，此处省略)*
它通过**低矮的轿跑SUV造型**和**极致的空气动力学优化**，实现了性能与美学的平衡。同时，其**极简主义的外观**（如封闭式前脸、隐藏式门把手、无边框车门）和**独特的细节设计**（如贯穿式尾灯、星环轮毂），共同塑造出一种极具辨识度和未来感的视觉形象。这种设计不仅在外观上吸引人，也体现了小鹏汽车在智能电动化领域的技术实力和设计哲学。
A2: 根据您提供的图片，如果将“小车”理解为“火车头”，那么图中只有一辆小车。这辆车是小鹏G9，从侧面展示，车身呈银灰色，设计非常现代和流线型。

MindGPT-4ov-30B-A3B

A1: 这辆理想i6的设计非常独特，溜背造型，风阻系数低，运动感十足。前脸没有传统的进气格栅，车头部分的线条简洁而现代，与车身整体的流线型设计相协调，增强了车辆的动感和科技感。双色车身设计，视觉比例更和谐，好看、有层次。
A2：图中有一辆小火车，它由一个火车头和七个车厢组成，所以总共有八辆小车。

Sample-3 (Image Missing)

Question

Create the webpage using HTML and CSS based on my sketch design. Color it in dark mode.

MindGPT-4ov-30B-A3B

I'd be happy to help you create a dark-mode webpage based on your sketch design! However, I don't see an attached sketch or description of your design yet.
To get started, please provide one of the following:
A description of your sketch (e.g., "It has a header with a logo and navigation, a main content area with cards, and a footer")
A simple wireframe or sketch (you can describe it in text)
Key elements you want included (like buttons, images, forms, etc.)
Preferred layout (grid, columns, etc.)
Once I have that information, I'll create a complete HTML and CSS dark-mode webpage for you.
In the meantime, here's a basic dark-mode template you can use as a starting point:
<code...> *(code omitted)*

Qwen3-VL-30B-A3B

This HTML/CSS code creates a complete dark mode webpage with:
1. A sleek, modern dark theme using deep blacks and subtle accents
2. Responsive design that works on all device sizes
3. A navigation header with logo and menu
4. Hero section with call-to-action button
5. Feature cards highlighting key benefits of dark mode
6. Content sections with detailed information
7. Footer with contact information and social links

The color scheme uses:
- Primary background: #121212 (deep black)
- Secondary background: #1e1e1e (slightly lighter black)
- Accent color: #bb86fc (purple/lavender for highlights)
- Text colors: White and light gray for readability
- Card backgrounds: #2d2d2d (for visual separation)

All interactive elements have hover effects for better user experience, and the layout is fully responsive for mobile devices.
<code...> *(code omitted)*

Sample-4 (Image Missing)

Question

图中左前方桌子上有几个苹果和香蕉？

Qwen3-VL-30B-A3B

根据您提供的图片，左前方的桌子上有一个苹果和一个香蕉。所以，桌上有 1个苹果 和 1个香蕉。

MindGPT-4ov-30B-A3B

由于我无法查看图片，我无法确定图中左前方桌子上有几个苹果和香蕉。如果您能提供更多的描述或信息，我会尽力帮助您解答。

Figure 12 Case comparisons of MindGPT-4ov-30B-A3B and Qwen3-VL-30B-A3B examples, focusing on three types of modality-biased question-answering scenarios: cross-modal inconsistency, context inconsistency, and missing images.

Instruction Following. On instruction-following (IFEval), the MindGPT-4ov series achieves scores that are close to the Qwen3-VL series. The 8B variant in particular outperforms the same-scale baseline, demonstrating robust instruction comprehension and generation consistency. It is also noteworthy that both MindGPT-4ov series exceed Qwen2.5-VL-72B's IFEval baseline of 83.0.

In summary, the multi-stage post-training approach presented in this report not only effectively enhances the model's multimodal understanding capabilities, but also successfully preserves and strengthens its language reasoning and knowledge expression abilities on pure text tasks.

6.3 Performance on Vertical Tasks

To comprehensively evaluate the outstanding performance of MindGPT-4ov in vertical tasks, we conduct extensive comparisons with the Qwen3-VL series model across multiple dimensions. The compared results demonstrate that MindGPT-4ov not only excels in vertical tasks but also shows significant improvement in user experience. Its key advantages include mastery of vertical domain question answering and superior performance in Chinese-language and modality-biased scenarios, as well as more diverse, concise, and accurate responses.

Vertical domain question answering. While maintaining high competitiveness in general capabilities, MindGPT-4ov also expands its knowledge in vertical domains. In practical applications, it effectively reduces hallucination problems caused by insufficient knowledge yet forced reasoning, while preserving strong cross-domain generalization capabilities. As shown in Fig. 9, when addressing questions involving new vertical domain knowledge, MindGPT-4ov provides accurate responses, whereas the baseline model Qwen3-VL lacks the ability to answer such questions accurately.

Chinese question answering. MindGPT-4ov also demonstrates superior performance in Chinese tasks. As shown in Fig. 10 (a), MindGPT-4ov outperforms others in both general Chinese question answering tasks and Chinese OCR document comprehension. Furthermore, the examples shown

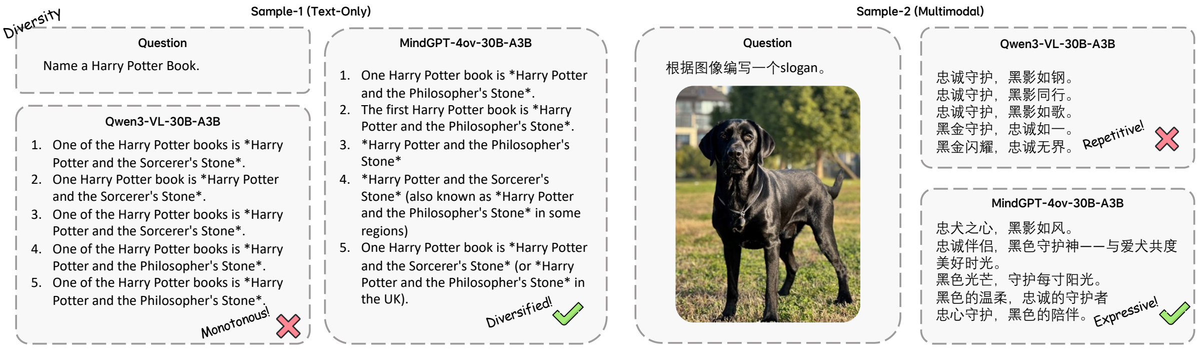

Name a Harry Potter Book.

1. One of the Harry Potter books is *Harry Potter and the Sorcerer's Stone*.
2. One Harry Potter book is *Harry Potter and the Sorcerer's Stone*.
3. One of the Harry Potter books is *Harry Potter and the Sorcerer's Stone*.
4. One of the Harry Potter books is *Harry Potter and the Philosopher's Stone*.
5. One of the Harry Potter books is *Harry Potter and the Philosopher's Stone*.

1. One Harry Potter book is *Harry Potter and the Philosopher's Stone*.
2. The first Harry Potter book is *Harry Potter and the Philosopher's Stone*.
3. *Harry Potter and the Philosopher's Stone*
4. *Harry Potter and the Sorcerer's Stone* (also known as *Harry Potter and the Philosopher's Stone* in some regions)
5. One Harry Potter book is *Harry Potter and the Sorcerer's Stone* (or *Harry Potter and the Philosopher's Stone* in the UK).

根据图像编写一个slogan。

忠诚守护，黑影如钢。
忠诚守护，黑影同行。
忠诚守护，黑影如歌。
黑金守护，忠诚如一。
黑金闪耀，忠诚无界。

忠犬之心，黑影如风。
忠诚伴侣，黑色守护神——与爱犬共度美好时光。
黑色光芒，守护每寸阳光。
黑色的温柔，忠诚的守护者
忠心守护，黑色的陪伴。

Figure 13 Case comparisons of MindGPT-4ov-30B-A3B and Qwen3-VL-30B-A3B, focusing on the diversity of responses.

in Fig. 11 indicate that MindGPT-4ov provides precise and focused reasoning in its responses, whereas Qwen3-VL generates redundant and logically flawed answers. This further confirms MindGPT-4ov's superior capability in Chinese question answering.

Modality-biased question answering. We further demonstrate the MindGPT-4ov's capabilities in cross-modal alignment, noise resistance, and factual output across three typical modality-biased question-answering scenarios: text-image inconsistency, context inconsistency, and missing images. By comparing the responses of MindGPT-4ov and Qwen3-VL on the same test samples, we evaluate the reliability and accuracy of the models in such challenging settings.

We further illustrate the proposed MindGPT-4ov's robustness to interference in three typical modality-biased question-answer scenarios: image–text inconsistency, contextual inconsistency, and missing images. By comparing the responses of MindGPT-4ov and Qwen3-VL on the same case, we evaluate the reliability and accuracy of MindGPT-4ov' outputs in modality-biased question-answer settings. As illustrated in Fig. 12, in Sample-1, which involves cross-modal inconsistency, MindGPT-4ov identifies the visual irrelevance, ignores the erroneous input image, and accurately answers the question. In Sample-2, which tests context irrelevance, MindGPT-4ov remains unaffected by unrelated interleaved context and correctly responds to both rounds of questions. In Sample-3 and Sample-4, which evaluate image-missing scenarios, MindGPT-4ov demonstrates stronger factual integrity by explicitly rejecting false outputs when no image is provided.

Diverse responses. We utilize NoveltyBench Zhang et al. (2025c) to measure the diversity of the models by counting the number of semantically distinct results generated in response to the same prompt, directly reflecting semantic diversity. As shown in Fig. 10 (b), MindGPT-4ov demonstrates improved performance on NoveltyBench. Furthermore, we present several cases to illustrate the greater diversity in MindGPT-4ov's responses. As depicted in Fig. 13, Qwen3-VL exhibits monotonicity in its replies, repeatedly using the "One of the Harry Potter books is..." with slight redundancy and repetition in expression, while lacking informational expansion. In contrast, MindGPT-4ov's responses avoid repetitive sentence structures and cover more dimensions of information.

Concise and accurate responses. An excellent MLLM must not only possess strong general capabilities but also can ensure that its interaction style aligns with human habits. In practical application evaluations, MindGPT-4ov demonstrates outstanding performance in both response accuracy and conciseness, delivering a more human-like interaction experience. When presented with the same input image and question, MindGPT-4ov can directly address the core of the query,

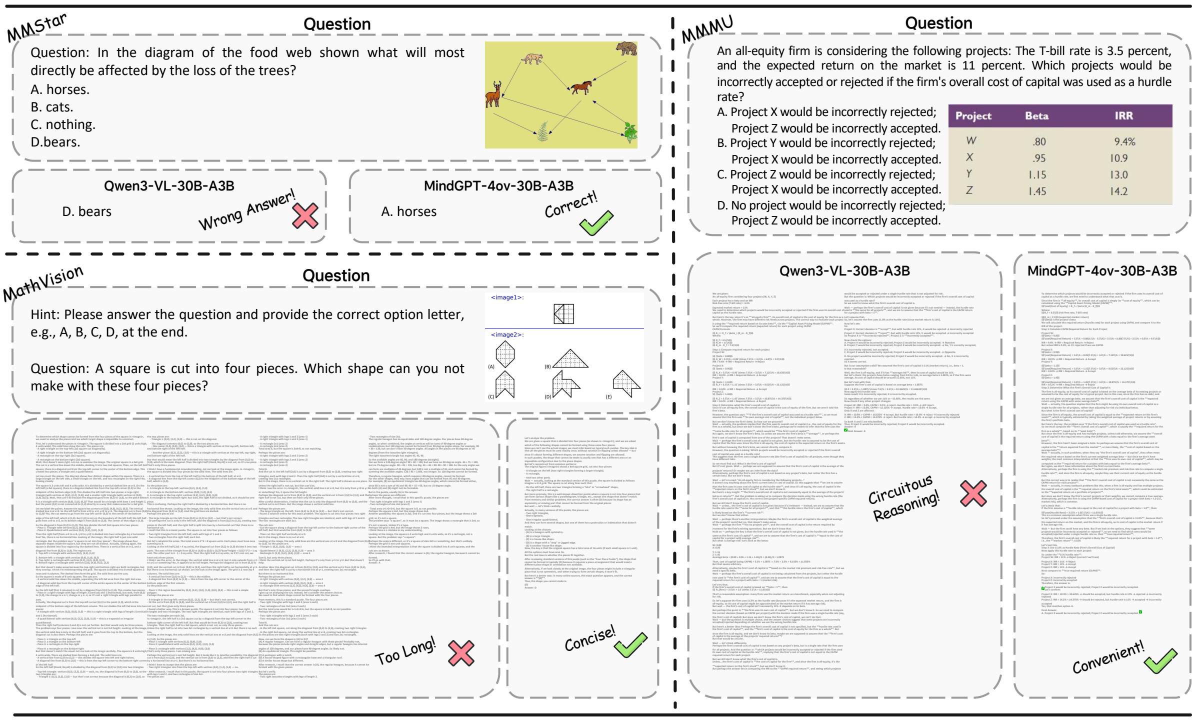

Question: In the diagram of the food web shown what will most directly be affected by the loss of the trees?
A. horses.
B. cats.
C. nothing.
D.bears.

D. bears

A. horses

Hint: Please answer the question and provide the correct option letter, e.g., A, B, C, D, at the end.

Question: A square is cut into four pieces. Which shape can you not make with these four pieces?

An all-equity firm is considering the following projects: The T-bill rate is 3.5 percent, and the expected return on the market is 11 percent. Which projects would be incorrectly accepted or rejected if the firm's overall cost of capital was used as a hurdle rate?
A. Project X would be incorrectly rejected; Project Z would be incorrectly accepted.
B. Project Y would be incorrectly rejected; Project X would be incorrectly accepted.
C. Project Z would be incorrectly rejected; Project X would be incorrectly accepted.
D. No project would be incorrectly rejected; Project Z would be incorrectly accepted.

Project	Beta	IRR
W	.80	9.4%
X	.95	10.9
Y	1.15	13.0
Z	1.45	14.2

Figure 14 Case comparisons of MindGPT-4ov-30B-A3B and Qwen3-VL-30B-A3B, focusing on the conciseness and accuracy of their response styles.

providing precise answers while effectively avoiding redundant details. In contrast, the baseline model Qwen3-VL often produces lengthy and irrelevant responses.

We showcase the advantages of MindGPT-4ov's user experience across multiple dimensions. For instance, as illustrated in Fig. 14, we collect examples from the general question-answering benchmark MMStar, the mathematical capability benchmark MathVision, and the STEM benchmark MMMU. These examples reveal that Qwen3-VL tends to generate excessively long responses with unnecessary background information, whereas MindGPT-4ov directly identifies the key points, offering concise and accurate descriptions along with correct answers. This human-like response characteristic significantly enhances interaction efficiency and user experience in real-world applications.

Furthermore, to objectively evaluate the conciseness and accuracy of MindGPT-4ov's responses, we compared the response length distributions of MindGPT-4ov-30B-A3B and Qwen3-VL-30B-A3B on MathVista. The results shown in Fig. 10 (c) indicate that MindGPT-4ov generates shorter responses while achieving an accuracy of 83.3 on MathVista, surpassing Qwen3-VL by 3.2%.

7 Conclusion

This paper proposes MindGPT-4ov, a systematic and end-to-end engineering framework for multimodal large language models tailored to vertical applications. The framework encompasses the entire pipeline of data management, model training, and deployment, aiming to effectively transfer the general capabilities of large multimodal models to vertical domains while mitigating catastrophic forgetting and enhancing user experience. By integrating information density-based data synthesis methods, collaborative curriculum supervised fine-tuning strategies, multi-stage hybrid reward reinforcement learning mechanisms, and efficient training and inference optimization techniques, MindGPT-4ov demonstrates significant advantages in both general and vertical tasks; its performance matches or even surpasses existing advanced multimodal large language models, while also exhibiting excellent user experience and system scalability. MindGPT-4ov is a reproducible, scalable approach for vertical-domain customization that requires no changes to the underlying architecture of pretrained general multimodal large language models, which enables seamless transfer from general capabilities to vertical applications.

8 Contributions

All contributors of this work are listed in alphabetical order by their last names.

Core Contributors: Chaoqun Du, Feng Gu, Wei He, Qizhen Li, Zide Liu, Xuhao Pan, Chang Ren, Xudong Rao, Chenfeng Wang, Chengjun Yu, Yufei Zheng, Chunpeng Zhou, Xuhan Zhu

Contributors: Jiawei Chen, Xingru Chen, Handong Cui, Li Gong, Maokui He, Yi Hu, Tianyu Lan, Hengtao Li, Shanshan Li, Xiaobo Liu, Hongli Luo, Jing Luo, Hao Ma, Ning Mao, Lifu Mu, Zhiheng Qu, Tong Sun, Xintian Shen, Haoyi Sun, Qian Wang, Wei Wang, Xin Wang, Lian Wen, Zhichao Wang, Shuo Xie, Hongfu Yang, Jiajun Yang, Shengyu Yao, Mi Yuan, Jiqing Zhan, Hongyuan Zhang, Qi Zhang, Lihao Zheng, Zheng Zhou, Jiaxu Zhu, Yun Zhu

Project Leaders: Tao Wei, Pengfei Yu

Supervisors: Wei Chen, Pan Zhou

References

Aime, 2024. URL `https://maa.org/maa-invitational-competitions/`.

Math500, 2024. URL `https://artificialanalysis.ai/evaluations/math-500`.

Ops-mm-embedding-v1-7b, 2025. URL `"https://huggingface.co/OpenSearch-AI/Ops-MM-embedding-v1-7B"`.

Gpt-5 system card, 2025. URL `"https://cdn.openai.com/gpt-5-system-card.pdf"`.

Amey Agrawal, Ashish Panwar, Jayashree Mohan, Nipun Kwatra, Bhargav S Gulavani, and Ramachandran Ramjee. Sarathi: Efficient llm inference by piggybacking decodes with chunked prefills. arXiv preprint arXiv:2308.16369, 2023.

Jinze Bai, Shuai Bai, Shusheng Yang, Shijie Wang, Sinan Tan, Peng Wang, Junyang Lin, Chang Zhou, and Jingren Zhou. Qwen-vl: A versatile vision-language model for understanding, localization, text reading, and beyond. arXiv preprint arXiv:2308.12966, 2023.

Shuai Bai, Yuxuan Cai, Ruizhe Chen, Keqin Chen, Xionghui Chen, Zesen Cheng, Lianghao Deng, Wei Ding, Chang Gao, Chunjiang Ge, Wenbin Ge, et al. Qwen3-vl technical report. arXiv preprint arXiv:2511.21631, 2025a.

Shuai Bai, Keqin Chen, Xuejing Liu, Jialin Wang, Wenbin Ge, Sibo Song, Kai Dang, Peng Wang, Shijie Wang, Jun Tang, et al. Qwen2.5-vl technical report. arXiv:2502.13923, 2025b.

Weilin Cai, Juyong Jiang, Fan Wang, Jing Tang, Sunghun Kim, and Jiayi Huang. A survey on mixture of experts in large language models. IEEE Transactions on Knowledge and Data Engineering, 2025a.

Wenxiao Cai, Iaroslav Ponomarenko, Jianhao Yuan, Xiaoqi Li, Wankou Yang, Hao Dong, and Bo Zhao. Spatialbot: Precise spatial understanding with vision language models. In 2025 IEEE International Conference on Robotics and Automation (ICRA), pages 9490–9498. IEEE, 2025b.

Yuji Cao, Huan Zhao, Yuheng Cheng, Ting Shu, Yue Chen, Guolong Liu, Gaoqi Liang, Junhua Zhao, Jinyue Yan, and Yun Li. Survey on large language model-enhanced reinforcement learning: Concept, taxonomy, and methods. IEEE Transactions on Neural Networks and Learning Systems, 2024.

Boyuan Chen, Zhuo Xu, Sean Kirmani, Brain Ichter, Dorsa Sadigh, Leonidas Guibas, and Fei Xia. Spatialvlm: Endowing vision-language models with spatial reasoning capabilities. In Proceedings of the IEEE/CVF Conference on Computer Vision and Pattern Recognition, pages 14455–14465, 2024a.

Jiankang Chen, Tianke Zhang, Changyi Liu, Haojie Ding, Yaya Shi, Huihui Xiao, Bin Wen, Fan Yang, Tingting Gao, Di ZHANG, et al. Taskgalaxy: Scaling multi-modal instruction fine-tuning with tens of thousands vision task types. In The Thirteenth International Conference on Learning Representations.

Lin Chen, Jinsong Li, Xiaoyi Dong, Pan Zhang, Yuhang Zang, Zehui Chen, Haodong Duan, Jiaqi Wang, Yu Qiao, Dahua Lin, et al. Are we on the right way for evaluating large vision-language models? In NeurIPS, 2024b.

Zhipeng Chen, Xiaobo Qin, Youbin Wu, Yue Ling, Qinghao Ye, Wayne Xin Zhao, and Guang Shi. Pass@ k training for adaptively balancing exploration and exploitation of large reasoning models. arXiv preprint arXiv:2508.10751, 2025.

Gheorghe Comanici, Eric Bieber, Mike Schaekermann, Ice Pasupat, Noveen Sachdeva, Inderjit Dhillon, Marcel Blistein, Ori Ram, Dan Zhang, Evan Rosen, et al. Gemini 2.5: Pushing the frontier with advanced reasoning, multimodality, long context, and next generation agentic capabilities. arXiv:2507.06261, 2025.

X.AI Corp. Grok-1.5 vision preview: Connecting the digital and physical worlds with our first multimodal model. `https://x.ai/blog/grok-1.5v`, 2024.

Haodong Duan, Junming Yang, Yuxuan Qiao, Xinyu Fang, Lin Chen, Yuan Liu, Xiaoyi Dong, Yuhang Zang, Pan Zhang, Jiaqi Wang, et al. Vlmevalkit: An open-source toolkit for evaluating large multi-modality models. In Proceedings of the 32nd ACM International Conference on Multimedia, pages 11198–11201, 2024.

Chaoyou Fu, Peixian Chen, Yunhang Shen, Yulei Qin, Mengdan Zhang, Xu Lin, Jinrui Yang, Xiawu Zheng, Ke Li, Xing Sun, et al. Mme: A comprehensive evaluation benchmark for multimodal large language models. arXiv:2306.13394, 2023.

Chaoyou Fu, Yuhan Dai, Yongdong Luo, Lei Li, Shuhuai Ren, Renrui Zhang, Zihan Wang, Chenyu Zhou, Yunhang Shen, Mengdan Zhang, et al. Video-mme: The first-ever comprehensive evaluation benchmark of multi-modal llms in video analysis. In Proceedings of the Computer Vision and Pattern Recognition Conference, pages 24108–24118, 2025.

Ling Fu, Biao Yang, Zhebin Kuang, Jiajun Song, Yuzhe Li, Linghao Zhu, Qidi Luo, Xinyu Wang, Hao Lu, Mingxin Huang, et al. Ocrbench v2: An improved benchmark for evaluating large multimodal models on visual text localization and reasoning, 2024b. URL https://arxiv.org/abs/2501.00321.

Xingyu Fu, Yushi Hu, Bangzheng Li, Yu Feng, Haoyu Wang, Xudong Lin, Dan Roth, Noah A Smith, Wei-Chiu Ma, and Ranjay Krishna. Blink: Multimodal large language models can see but not perceive. In European Conference on Computer Vision, pages 148–166. Springer, 2024.

Trevor Gale, Deepak Narayanan, Cliff Young, and Matei Zaharia. MegaBlocks: Efficient Sparse Training with Mixture-of-Experts. Proceedings of Machine Learning and Systems, 5, 2023.

Tianrui Guan, Fuxiao Liu, Xiyang Wu, Ruiqi Xian, Zongxia Li, Xiaoyu Liu, Xijun Wang, Lichang Chen, Furong Huang, Yaser Yacoob, et al. Hallusionbench: an advanced diagnostic suite for entangled language hallucination and visual illusion in large vision-language models. In Proceedings of the IEEE/CVF Conference on Computer Vision and Pattern Recognition, pages 14375–14385, 2024.

Daya Guo, Dejian Yang, Haowei Zhang, Junxiao Song, Ruoyu Zhang, Runxin Xu, Qihao Zhu, Shirong Ma, Peiyi Wang, Xiao Bi, et al. Deepseek-r1: Incentivizing reasoning capability in llms via reinforcement learning. arXiv preprint arXiv:2501.12948, 2025a.

Dong Guo, Faming Wu, Feida Zhu, Fuxing Leng, Guang Shi, Haobin Chen, Haoqi Fan, Jian Wang, Jianyu Jiang, Jiawei Wang, et al. Seed1. 5-vl technical report. arXiv:2505.07062, 2025b.

Pengcheng He, Xiaodong Liu, Jianfeng Gao, and Weizhu Chen. Deberta: Decoding-enhanced bert with disentangled attention. arXiv preprint arXiv:2006.03654, 2020.

Deepti Hegde, Rajeev Yasarla, Hong Cai, Shizhong Han, Apratim Bhattacharyya, Shweta Mahajan, Litian Liu, Risheek Garrepalli, Vishal M Patel, and Fatih Porikli. Distilling multi-modal large language models for autonomous driving. In Proceedings of the Computer Vision and Pattern Recognition Conference, pages 27575–27585, 2025.

Dan Hendrycks, Collin Burns, Steven Basart, Andy Zou, Mantas Mazeika, Dawn Song, and Jacob Steinhardt. Measuring massive multitask language understanding. arXiv preprint arXiv:2009.03300, 2020.

Wenyi Hong, Wenmeng Yu, Xiaotao Gu, Guo Wang, Guobing Gan, Haomiao Tang, Jiale Cheng, Ji Qi, Junhui Ji, Lihang Pan, et al. Glm-4.1 v-thinking: Towards versatile multimodal reasoning with scalable reinforcement learning. arXiv e-prints, pages arXiv–2507, 2025.

Lei Huang, Weijiang Yu, Weitao Ma, Weihong Zhong, Zhangyin Feng, Haotian Wang, Qianglong Chen, Weihua Peng, Xiaocheng Feng, Bing Qin, et al. A survey on hallucination in large language models: Principles, taxonomy, challenges, and open questions. ACM Transactions on Information Systems, 43(2):1–55, 2025.

Aaron Hurst, Adam Lerer, Adam P Goucher, Adam Perelman, Aditya Ramesh, Aidan Clark, AJ Ostrow, Akila Welihinda, Alan Hayes, Alec Radford, et al. Gpt-4o system card. arXiv preprint arXiv:2410.21276, 2024.

Edward L Ionides. Truncated importance sampling. Journal of Computational and Graphical Statistics, 17(2):295–311, 2008.

Aniruddha Kembhavi, Mike Salvato, Eric Kolve, Minjoon Seo, Hannaneh Hajishirzi, and Ali Farhadi. A diagram is worth a dozen images. In ECCV, 2016.

Alexander Kirillov, Eric Mintun, Nikhila Ravi, Hanzi Mao, Chloe Rolland, Laura Gustafson, Tete Xiao, Spencer Whitehead, Alexander C Berg, Wan-Yen Lo, et al. Segment anything. In ICCV, 2023.

Woosuk Kwon, Zhuohan Li, Siyuan Zhuang, Ying Sheng, Lianmin Zheng, Cody Hao Yu, Joseph Gonzalez, Hao Zhang, and Ion Stoica. Efficient memory management for large language model serving with pagedattention. In Proceedings of the 29th symposium on operating systems principles, pages 611–626, 2023.

Sicong Leng, Yun Xing, Zesen Cheng, Yang Zhou, Hang Zhang, Xin Li, Deli Zhao, Shijian Lu, Chunyan Miao, and Lidong Bing. The curse of multi-modalities: Evaluating hallucinations of large multimodal models across language, visual, and audio. arXiv preprint arXiv:2410.12787, 2024.

Kunchang Li, Yali Wang, Yinan He, Yizhuo Li, Yi Wang, Yi Liu, Zun Wang, Jilan Xu, Guo Chen, Ping Luo, et al. Mvbench: A comprehensive multi-modal video understanding benchmark. In Proceedings of the IEEE/CVF Conference on Computer Vision and Pattern Recognition, pages 22195–22206, 2024.

Tianjian Li, Yiming Zhang, Ping Yu, Swarnadeep Saha, Daniel Khashabi, Jason Weston, Jack Lanchantin, and Tianlu Wang. Jointly reinforcing diversity and quality in language model generations. arXiv preprint arXiv:2509.02534, 2025a.

Zichao Li, Xueru Wen, Jie Lou, Yuqiu Ji, Yaojie Lu, Xianpei Han, Debing Zhang, and Le Sun. The devil is in the details: Tackling unimodal spurious correlations for generalizable multimodal reward models. arXiv preprint arXiv:2503.03122, 2025b.

Zichao Li, Xueru Wen, Jie Lou, Yuqiu Ji, Yaojie Lu, Xianpei Han, Debing Zhang, and Le Sun. The devil is in the details: Tackling unimodal spurious correlations for generalizable multimodal reward models. arXiv preprint arXiv:2503.03122, 2025c.

Tianwei Lin, Wenqiao Zhang, Sijing Li, Yuqian Yuan, Binhe Yu, Haoyuan Li, Wanggui He, Hao Jiang, Mengze Li, Xiaohui Song, et al. Healthgpt: A medical large vision-language model for unifying comprehension and generation via heterogeneous knowledge adaptation. arXiv preprint arXiv:2502.09838, 2025.

Liyuan Liu, Feng Yao, Dinghuai Zhang, Chengyu Dong, Jingbo Shang, and Jianfeng Gao. Flashrl: 8bit rollouts, full power rl, August 2025a. URL `https://fengyao.notion.site/flash-rl`.

Mingjie Liu, Shizhe Diao, Jian Hu, Ximing Lu, Xin Dong, Hao Zhang, Alexander Bukharin, Shaokun Zhang, Jiaqi Zeng, Makesh Narsimhan Sreedhar, et al. Scaling up rl: Unlocking diverse reasoning in llms via prolonged training. arXiv preprint arXiv:2507.12507, 2025b.

Xianjie Liu, Yiman Hu, Yixiong Zou, Liang Wu, Jian Xu, and Bo Zheng. Hide: Rethinking the zoom-in method in high resolution mllms via hierarchical decoupling. arXiv preprint arXiv:2510.00054, 2025c.

Yuliang Liu, Zhang Li, Mingxin Huang, Biao Yang, Wenwen Yu, Chunyuan Li, Xu-Cheng Yin, Cheng-Lin Liu, Lianwen Jin, and Xiang Bai. Ocrbench: on the hidden mystery of ocr in large multimodal models. Science China Information Sciences, 2024.

Alejandro Lozano, Min Woo Sun, James Burgess, Liangyu Chen, Jeffrey J Nirschl, Jeffrey Gu, Ivan Lopez, Josiah Aklilu, Anita Rau, Austin Wolfgang Katzer, et al. Biomedica: An open biomedical image-caption archive, dataset, and vision-language models derived from scientific literature. In Proceedings of the Computer Vision and Pattern Recognition Conference, pages 19724–19735, 2025.

Pan Lu, Hritik Bansal, Tony Xia, Jiacheng Liu, Chunyuan Li, Hannaneh Hajishirzi, Hao Cheng, Kai-Wei Chang, Michel Galley, and Jianfeng Gao. Mathvista: Evaluating mathematical reasoning of foundation models in visual contexts. In ICLR, 2024.

Minesh Mathew, Dimosthenis Karatzas, and CV Jawahar. Docvqa: A dataset for vqa on document images. In WACV, 2021.

Minesh Mathew, Viraj Bagal, Rubèn Tito, Dimosthenis Karatzas, Ernest Valveny, and CV Jawahar. Infographicvqa. In WACV, 2022.

Deepak Narayanan, Mohammad Shoeybi, Jared Casper, Patrick LeGresley, Mostofa Patwary, Vijay Korthikanti, Dmitri Vainbrand, Prethvi Kashinkunti, Julie Bernauer, Bryan Catanzaro, et al. Efficient large-scale language model training on gpu clusters using megatron-lm. In Proceedings of the international conference for high performance computing, networking, storage and analysis, pages 1–15, 2021.

Junbo Niu, Zheng Liu, Zhuangcheng Gu, Bin Wang, Linke Ouyang, Zhiyuan Zhao, Tao Chu, Tianyao He, Fan Wu, Qintong Zhang, et al. Mineru2. 5: A decoupled vision-language model for efficient high-resolution document parsing. arXiv preprint arXiv:2509.22186, 2025.

Roni Paiss, Ariel Ephrat, Omer Tov, Shiran Zada, Inbar Mosseri, Michal Irani, and Tali Dekel. Teaching clip to count to ten. In ICCV, 2023.

Yusu Qian, Hanrong Ye, Jean-Philippe Fauconnier, Peter Grasch, Yinfei Yang, and Zhe Gan. Mia-bench: Towards better instruction following evaluation of multimodal llms. arXiv preprint arXiv:2407.01509, 2024.

Rafael Rafailov, Archit Sharma, Eric Mitchell, Christopher D Manning, Stefano Ermon, and Chelsea Finn. Direct preference optimization: Your language model is secretly a reward model. Advances in neural information processing systems, 36:53728–53741, 2023.

David Rein, Betty Li Hou, Asa Cooper Stickland, Jackson Petty, Richard Yuanzhe Pang, Julien Dirani, Julian Michael, and Samuel R Bowman. Gpqa: A graduate-level google-proof q&a benchmark. In First Conference on Language Modeling, 2024.

Christoph Schuhmann, Richard Vencu, Romain Beaumont, Robert Kaczmarczyk, Clayton Mullis, Aarush Katta, Theo Coombes, Jenia Jitsev, and Aran Komatsuzaki. Laion-400m: Open dataset of clip-filtered 400 million image-text pairs. arXiv preprint arXiv:2111.02114, 2021.

Zhihong Shao, Peiyi Wang, Qihao Zhu, Runxin Xu, Junxiao Song, Xiao Bi, Haowei Zhang, Mingchuan Zhang, YK Li, Yang Wu, et al. Deepseekmath: Pushing the limits of mathematical reasoning in open language models. arXiv preprint arXiv:2402.03300, 2024.

Wei Shen, Jiangbo Pei, Yi Peng, Xuchen Song, Yang Liu, Jian Peng, Haofeng Sun, Yunzhuo Hao, Peiyu Wang, Jianhao Zhang, et al. Skywork-r1v3 technical report. arXiv preprint arXiv:2507.06167, 2025.

Yuda Song, Julia Kempe, and Remi Munos. Outcome-based exploration for llm reasoning. arXiv preprint arXiv:2509.06941, 2025.

Kimi Team, Angang Du, Bohong Yin, Bowei Xing, et al. Kimi-vl technical report, 2025.

Xiaoyu Tian, Junru Gu, Bailin Li, Yicheng Liu, Yang Wang, Zhiyong Zhao, Kun Zhan, Peng Jia, Xianpeng Lang, and Hang Zhao. Drivevlm: The convergence of autonomous driving and large vision-language models. arXiv preprint arXiv:2402.12289, 2024.

SMTI Tonmoy, SM Zaman, Vinija Jain, Anku Rani, Vipula Rawte, Aman Chadha, and Amitava Das. A comprehensive survey of hallucination mitigation techniques in large language models. arXiv preprint arXiv:2401.01313, 6, 2024.

Fei Wang, Xingyu Fu, James Y Huang, Zekun Li, Qin Liu, Xiaogeng Liu, Mingyu Derek Ma, Nan Xu, Wenxuan Zhou, Kai Zhang, et al. Muirbench: a comprehensive benchmark for robust multi-image understanding (2024). URL https://arxiv. org/abs/2406.09411.

Ke Wang, Junting Pan, Weikang Shi, Zimu Lu, Mingjie Zhan, and Hongsheng Li. Measuring multimodal mathematical reasoning with math-vision dataset. In NeurIPS, 2024a.

Peng Wang, Shuai Bai, Sinan Tan, Shijie Wang, Zhihao Fan, Jinze Bai, Keqin Chen, Xuejing Liu, Jialin Wang, Wenbin Ge, et al. Qwen2-vl: Enhancing vision-language model's perception of the world at any resolution. arXiv:2409.12191, 2024b.

Weiyun Wang, Zhangwei Gao, Lixin Gu, Hengjun Pu, Long Cui, Xingguang Wei, Zhaoyang Liu, Linglin Jing, Shenglong Ye, Jie Shao, et al. Internvl3.5: Advancing open-source multimodal models in versatility, reasoning, and efficiency. arXiv preprint arXiv:2508.18265, 2025a.

Yubo Wang, Xueguang Ma, Ge Zhang, Yuansheng Ni, Abhranil Chandra, Shiguang Guo, Weiming Ren, Aaran Arulraj, Xuan He, Ziyan Jiang, et al. Mmlu-pro: A more robust and challenging multi-task language understanding benchmark. Advances in Neural Information Processing Systems, 37:95266–95290, 2024c.

Zhaowei Wang, Wenhao Yu, Xiyu Ren, Jipeng Zhang, Yu Zhao, Rohit Saxena, Liang Cheng, Ginny Wong, Simon See, Pasquale Minervini, et al. Mmlongbench: Benchmarking long-context vision-language models effectively and thoroughly. arXiv preprint arXiv:2505.10610, 2025b.

Penghao Wu and Saining Xie. V*: Guided visual search as a core mechanism in multimodal llms. In CVPR, 2024.

Feng Yao, Liyuan Liu, Dinghuai Zhang, Chengyu Dong, Jingbo Shang, and Jianfeng Gao. Your efficient rl framework secretly brings you off-policy rl training, August 2025. URL `https://fengyao.notion.site/off-policy-rl`.

Zihao Ye, Lequn Chen, Ruihang Lai, Wuwei Lin, Yineng Zhang, Stephanie Wang, Tianqi Chen, Baris Kasikci, Vinod Grover, Arvind Krishnamurthy, and Luis Ceze. Flashinfer: Efficient and customizable attention engine for llm inference serving. arXiv preprint arXiv:2501.01005, 2025. URL `https://arxiv.org/abs/2501.01005`.

Qiying Yu, Zheng Zhang, Ruofei Zhu, Yufeng Yuan, Xiaochen Zuo, Yu Yue, Weinan Dai, Tiantian Fan, Gaohong Liu, Lingjun Liu, et al. Dapo: An open-source llm reinforcement learning system at scale. arXiv preprint arXiv:2503.14476, 2025.

Xiang Yue, Yuansheng Ni, Kai Zhang, Tianyu Zheng, Ruoqi Liu, Ge Zhang, Samuel Stevens, Dongfu Jiang, Weiming Ren, Yuxuan Sun, et al. Mmmu: A massive multi-discipline multimodal understanding and reasoning benchmark for expert agi. In CVPR, 2024.

Xiang Yue, Tianyu Zheng, Yuansheng Ni, Yubo Wang, Kai Zhang, Shengbang Tong, Yuxuan Sun, Ming Yin, Botao Yu, Ge Zhang, et al. Mmmu-pro: A more robust multi-discipline multimodal understanding benchmark. In ACL, 2025a.

Yang Yue, Zhiqi Chen, Rui Lu, Andrew Zhao, Zhaokai Wang, Shiji Song, and Gao Huang. Does reinforcement learning really incentivize reasoning capacity in llms beyond the base model? arXiv preprint arXiv:2504.13837, 2025b.

Kaiyan Zhang, Yuxin Zuo, Bingxiang He, Youbang Sun, Runze Liu, Che Jiang, Yuchen Fan, Kai Tian, Guoli Jia, Pengfei Li, et al. A survey of reinforcement learning for large reasoning models. arXiv preprint arXiv:2509.08827, 2025a.

Xiangxiang Zhang, Jingxuan Wei, Donghong Zhong, Qi Chen, Caijun Jia, Cheng Tan, Jinming Gu, Xiaobo Qin, Zhiping Liu, Liang Hu, et al. Structvrm: Aligning multimodal reasoning with structured and verifiable reward models. arXiv preprint arXiv:2508.05383, 2025b.

Yiming Zhang, Harshita Diddee, Susan Holm, Hanchen Liu, Xinyue Liu, Vinay Samuel, Barry Wang, and Daphne Ippolito. Noveltybench: Evaluating language models for humanlike diversity. arXiv preprint arXiv:2504.05228, 2025c.

Chujie Zheng, Shixuan Liu, Mingze Li, Xiong-Hui Chen, Bowen Yu, Chang Gao, Kai Dang, Yuqiong Liu, Rui Men, An Yang, et al. Group sequence policy optimization. arXiv preprint arXiv:2507.18071, 2025.

Yinmin Zhong, Shengyu Liu, Junda Chen, Jianbo Hu, Yibo Zhu, Xuanzhe Liu, Xin Jin, and Hao Zhang. {DistServe}: Disaggregating prefill and decoding for goodput-optimized large language model serving. In 18th USENIX Symposium on Operating Systems Design and Implementation (OSDI 24), pages 193–210, 2024.

Jeffrey Zhou, Tianjian Lu, Swaroop Mishra, Siddhartha Brahma, Sujoy Basu, Yi Luan, Denny Zhou, and Le Hou. Instruction-following evaluation for large language models. arXiv preprint arXiv:2311.07911, 2023.

Weijie Zhou, Manli Tao, Chaoyang Zhao, Haiyun Guo, Honghui Dong, Ming Tang, and Jinqiao Wang. Physvlm: Enabling visual language models to understand robotic physical reachability. In Proceedings of the Computer Vision and Pattern Recognition Conference, pages 6940–6949, 2025.

Jinguo Zhu, Weiyun Wang, Zhe Chen, Zhaoyang Liu, Shenglong Ye, Lixin Gu, Hao Tian, Yuchen Duan, Weijie Su, Jie Shao, et al. Internvl3: Exploring advanced training and test-time recipes for open-source multimodal models. arXiv:2504.10479, 2025.